National University of Lesotho

Evaluation and optimisation of solar water pumping systems for Lesotho

Itumeleng Moses Moholo

A dissertation submitted in partial fulfillment

of the requirements for the degree of

Master of Science in Sustainable Energy

Offered by the

Energy Research Centre

Faculty of Science & Technology

MAY 2020

ABSTRACT

Water and energy are the key drivers of sustainable development, yet the world is facing severe energy and water crisis. Photovoltaic water pumping system (PVWPS) is a mature technology that conserves both energy and water for sustainable applications. However the wider application of this technology is affected by improper system designs wider application of this technology is affected by improper system designs, high initial costs lack and of predictability . This study aims to evaluate critical factors for optimal sizing and performance prediction of PVWPS at the least cost of pumping. First objective of this study is to develop the meteorological parameters interpolated grid data base for Lesotho. Solar and ambient temperature data are recorded for 0.25 ×0.25 longitude and latitude interval for the range 27.00 East to 30.00 East and 28.00 South to 31.00 South. The range defines the extreme longitude and latitude boundaries of Lesotho. Grid data is interpolated and implemented into the computer program, hence meteorological parameters variations are automatically read at any point in Lesotho. Another objective is to develop a flow-power function, which comprehensively takes into account the instantaneous variation of ambient temperatures and solar irradiance and their effect on the pump system flow-rate and the system resistance. The flow-power function expresses the flow output of the solar pumping system as a function of the dynamic variation of the photovoltaic array power output, for a given pump and pipe parameters. The PVWPS components namely, the pump; solar photovoltaic array; pipeline system and the water storage are sized in an integrated fashion. The model is especially suitable for long pipelines where the PV array power required to deliver a demanded daily volume of water significantly decreases as the pumping main pipe diameter is increased. From the factory gate to site of installation the relative specific costs of PV array, pump and pipe differ from place to place. As a final objective an economical optimum combination of these sub system components, which meet the required daily demand of water at the least cost of pumping, is attained. Applying a time-step balance of the hourly pump flow output with the hourly water demand also enables a more precise estimation of the required balancing storage, by applying the mass-balance-curve approach. This study shows; how does the time step variation in meteorological parameters for a specified water requirement affect PVWP systems design and efficiencies; and how can the different pump-pipe combinations of PVWP systems be optimized from an integrated system perspective to arrive at the least cost of pumping. The applied method is technical accurate for sizing and also more economical thus proves to be a significant improvement to the traditional simplified approach of sizing solar pumping systems. It can result in significantly reduced unit cost of pumping. In the case study for Tosing, Lesotho (*27.90 longitude 30.36 latitude)* potable water demand of 350m^3/ day. The design overall system efficiency is 7.1% the required PV array power was reduced by 25.8 % and the required water storage capacity reduced by 50% when compared to their respective values prescribed by the traditional sizing method.

Keywords: *meteorological grid data base, dynamic variations, photovoltaic water pumping system (PVWPS), flow-power function, optimal sizing, least cost of pumping*.

ACKNOWLEDGEMENTS

This master's thesis was conducted at the National University of Lesotho – Energy Research Centre NUL-ERC. I gratefully acknowledge the institute and National Manpower Development Secretariat for financial support to persuade my studies.

First and foremost, I am deeply grateful to my supervisor Engineer Tawanda Hove for giving me the opportunity to work on this project, his continuous and invaluable guidance, support, motivation, and all the great experiences I had during my studies. It has been an honor to be one of NUL-ERC students. My deep and sincere gratitude goes to all ERC members for this humble experience especially our coordinator Doctor Moeketsi Mpholo. I thank all my facilitators and my dear colleagues.

Finally, I feel very much indebted to my family, and to almighty Father and Mother of creation for life.

DECLARATION

I declare that this dissertation, submitted for the degree of masters in Sustainable energy at the National University of Lesotho (NUL); Energy Research Centre (ERC) it is my own work and has not been previously submitted by me or anyone else for the degree at any other University. All the sources quoted have been acknowledged by references.

SIGNATURE: 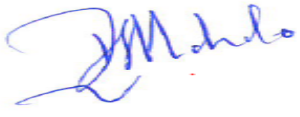

TABLE OF CONTENTS

LIST OF FIGURES

List of tables

NOMENCLATURE

Abbreviation

AC -alternate current

DC - direct current

Capex –capital expenditure

PV – photovoltaic

PWPS - photovoltaic water pumping system

O&M - operations and maintenance

$\eta_{overall}$ - overall system efficiency (%)

η_{pump}- pump efficiency (%)

η_{STC} - PV operating efficiency at standard test conditions

P_{STC} -PV Array at standard test conditions

P_{pv} -required PV power

η_{pv}- PV module efficiency (%)

Fm - matching factor

β -cell efficiency temperature coefficient

T_{cell} -cell temperature

$T_{c, NOCT}$ - nominal operating cell temperature (NOCT)

$T_{a, NOCT}$ -ambient temperature at NOCT

$G_{T, NOCT}$ -is the irradiance at NOCT

φ -tilt angle

G_T - global solar radiation on the tilted surface (W/m2)

G_d -diffuse horizontal solar radiation (W/m2)

G_b-global horizontal solar radiation (kW/m2)

$\bar{H}$- monthly- average daily irradiation.

$\bar{H}_h$ - monthly-average daily irradiation on a horizontal plane

$\bar{H}_d$ - monthly-average daily diffuse irradiation

$\bar{K}_h$ - monthly average clearness index

$\bar{G}_h$ -monthly-average hourly values for hourly global radiation on a horizontal plane

$\bar{G}_d$ -monthly-average hourly values for hourly diffuse radiation on a horizontal plane

ρ - water density (kg/m^3)

$\bar{\eta}_{pv}$ - average PV array efficiency (%)

$\bar{\eta}_{pump\_op}$-average pump efficiency (%)

$\bar{\eta}_{total}$ - overall electric-to-hydraulic efficiency (%)

g- gravity acceleration (9.8m/s^2)

TDH- total dynamic head (m)

H_O- static head (m)

P_{hyd} -hydraulic power

TDH_{op} - total dynamic head at operating point

Q_{op} - operating flow rate

CHAPTER 1: INTRODUCTION

1.1 Background

Water plays a vital role for all living organisms and major ecosystems as well as for human health, food production and economic development. Access to clean water is an essential necessity for the well-being of all people. Water availability has been identified as an important environmental constraint on development and ultimately a limiting factor for population growth and food production [1]. A standard solar (photovoltaic) water pumping system (PVWPS) has the potential to bring sustainable supplies of potable water to millions of people in developing countries to their numerous small villages and farms, where is in not economically feasible to extend the electrical national grid. [2].

Lesotho is a small land locked mountainous country completely surrounded by the Republic of South Africa. It has a total area of about 30 350km^2, a north-south extent of about 230km and a maximum width of about 210km. Lesotho is the only country in the world that is entirely situated above 1400m in altitude [3]. Water resources, surface and ground water, are abundant in Lesotho. The average rainfall is 760mm per annum, varying from 300mm per annum in the western lowlands to 1600mm per annum in the north eastern highlands [4].

Despite the availability of water; effective distribution of water is a major problem in Lesotho. Water is not always where it can readily be used. Due to the geographical situation, most of the water flows from the country. Lesotho's total renewable water resources are estimated to exceed 5031 Million m^3/year, yet Lesotho struggles to accesses water for communities and for industrial developments. There is a need of sustainable energy systems to deliver water from point of source to demand point, as most surface water is often found in the valleys, but it is slightly below the level of lands, and therefore requires being pumped [4].

The poverty reduction strategy and action plan of Lesotho is a document that underlines the commitment and strategies of the Lesotho Government to reduce poverty and the challenges relating to it. Its overall goal is to reduce poverty by more than 50% by 2015 and ultimately eradicate it by 2022 [5]. Water is seen as the first priority under the poverty reduction strategy and action plan. Hereby the poor are empowered to generate income and through the promotion of productive uses of water in the rural areas [5].

The long term water and sanitation strategy of Lesotho (2014), is a framework for utilizing and managing water resource in Lesotho [6]. It states that all water found naturally in the country belongs to

the Basotho nation. The objectives of the Lesotho Water and Sanitation Policy (LWSP) are to promote: (1) The proper management of the country's water resources and its sustainable utilization; (2) Adequate and sustainable supply of potable water and sanitation services to all of the population of Lesotho; (3) Co-ordination and coherence in the management and development of water and other related natural resources, in order to maximize the resultant socio-economic benefits with-out compromising the sustainability of vital ecosystems [6].

Thus the maximum utilization of water in Lesotho for sustainable socio-economic development requires energy systems that are sustainable and efficient. The current energy policy of Lesotho is designed specifically to be a guiding tool to solve problems endured by energy sector in Lesotho. The availability of renewable energy resources and the current energy market conditions of Lesotho are key parameters in formulation of the current policy. It states that the rural electrification unit shall establish, from energy master plan, strategies to deploy off-grid solutions and rank criteria of locations also to promote cost competitive off grid solutions [7].

Local market conditions that obstacle the attainment of access to electrification in Lesotho and Sub-Sahara African region are the sparsely distributed population, remoteness of communities and socio–economic factors including; low income consumers with high cost of energy infrastructure and the lack of skilled human capital and limited financial capital. These socioeconomic factors are mapped with availability of renewable energy resources, to assess local energy market conditions, for sustainable energy systems [8].

Solar radiation data indicates that the country has an abundant solar energy resource, with more than 300 days of sunshine per year. The duration of sunshine ranges from 10.2 to 13.8 hours per day for both the highlands and the lowlands, with a high level of solar radiation regime at an average of 5.4–6.7 kWh/m^2/day on the horizontal surface [9]. Cold temperatures and high altitude provide advantages, for photovoltaic modules tend to produce higher voltage as the temperature drops and, conversely, to lose voltage in high temperatures. High altitudes can give an advantage of enhanced-irradiance due to reduced "air-mass".

Unfortunately, in many cases the application of the solar water pump technology ignores the social, environmental and economic conditions of the location, leading to inadequate system and ultimately the failure of the project. The mismatch between water demand and supply pattern has a major effect on economic viability of the PV pumping systems and thus required to be examined seriously [10]

Another important fact of the analysis of a photovoltaic (PV) system is usually the required economic investment. Sometimes an interesting project does not have any future because of the economical

investment that is bigger than the incoming profits, so it is important to know before developing if it is economically viable or not. PV system viability is sensitive to solar irradiation availability at the location where the pump is installed [11]. An increase in the amount of solar irradiation also increases the flow rate and efficiency of PVWPS. If the system's output is not fully utilized then the installation may not be financially attractive. The economic success of the photovoltaic systems deployment is related to its financial viability, which depends on the capacity to generating energy at a competitive cost [12].

1.2 Knowledge gaps and challenges

In Lesotho, the majority of the population still resides in rural areas where settlements are normally scattered and in geographical places difficult to reach due to the mountainous terrain. This makes it very costly to extend the national grid to such communities with no returns on capital investment as the consumption is bound to be very low due to higher rates of unemployment in rural areas which result in cost of electricity being unaffordable [13]. The low electrification rate in rural areas prevents access to energy services which are essential to improve living conditions. One of these energy services is electrified water pumping system, which is particularly relevant for these areas where water access continues being a significant challenge.

Pumping systems powered by photovoltaic energy have emerged as an interesting solution in off-grid areas. However the degree of acceptance of photovoltaic solar water pumping systems by the users is very low. There are several factors which have inhibited the wide-spread implementation of these systems. These include the high initial cost, lack of awareness and technical expertise (improper designs), lack of sufficient knowledge on the daily output of these systems (predictability) and a history of failures [14]. These systems have experienced problems, mainly because they were not properly sized. The output in terms of the daily volume of water pumped was below the expectation of the users or oversized, thus increasing the costs [15].

As contribution to knowledge this thesis represents a first attempt at studying the sustainability of PVWPS technology for access to clean, affordable, reliable water and energy services, supporting the sustainable development objectives of rural communities in Lesotho. This study will demonstrate a methodology of how to size, optimize, and predict the long term performance of the PVWPS; for technically and socio-economically feasible PVWPS applications in Lesotho. Most scientific research carried out in this field were focused on system design, optimization of system components (such as power conditioning systems and performance improvement of the solar array), and technical and economic comparisons between PV and other standalone power sources. However, there is a knowledge gap in the systematic optimization of energysystems, when considering water requirement, solar resource variability, and water demand

conditions. System failures and corresponding economic losses still occur due to the inadequacy of system integration with the environment and socio-economic capacity. In most works done so far, PVWP systems have been considered as independent electric devices, without taking into consideration how the system is affected by the environment and how the system affects the environment (e.g., pumped water and specific water requirement). Thus, this thesis research questions are; **how does the time step variation in meteorological parameters for a specified water requirement affect PVWP systems design and efficiency**; and **how can the different pump-pipe combinations of PVWP systems be optimized from an integrated system perspective to arrive at the least cost of pumping?**

1.3 Purpose of the study.

The purpose of this study is to evaluate necessary parameters to consider when designing PVWPS in Lesotho, the study intends to inform stakeholders of the basic factors to consider when developing PVWPS programs in Lesotho. Reviewed studies concluded that; the main factors inhibiting widespread implementation of PV pumping technology are high initial capital cost and lack of awareness among users [15-16]. The study will contribute to implementation of solar water pumping systems projects that are designed on rational basis in Lesotho; that is technically efficient energy systems, socio-economically; reliable, affordable and environmentally sustainable energy and water services.

The study will again to research knowledge; a construction and demonstration the solar grid data base and interpolation program that are especially suitable for the widespread implementation of PVWPS technologies across the whole country. This study presents a methodology for optimally sizing PVWPS, for long-term system performance; that are technically and socio-economically sustainable. The study will moreover contribute to access to optimally priced pumping services. By optimisation of different system combinations, objective function of the least unit cost of pumping can be attained [17].

Another purpose of the study is to build stakeholders and users capacity to uptake solar pumping technology in all sectors (households, agriculture, mining and others) that require sustainable supply of water. It is apparent that sustainable application of this technology will contribute to solve socio challenges of water demand, improve health and wellbeing of Basotho, as well to support the implementation of poverty reduction strategies, for rural community development. Because if used for farming applications; solar pumping systems enhances important phenomena of basic life supporting systems of the food, water and energy nexus.

Poor technical and economic performance of these PVWPS is execrated by ignoring knowledge of location variables such as; water demand, inflation rate, discount rate, total cost of the system and the vertical and the horizontal distance from water source to discharge point and most crucial amount of

solar radiation. These parameters are site characteristics that require proper evaluation for optimal sizing of PVWPS. Thus this paper demonstrate specific case study that evaluate the effects of this parameters on efficiency of PVWPS and the economic feasibility of this technologies while satisfying user's objective [16].

The study also aims to optimize life cycle cost of PVWPS to improve PVWPS design to be more accurate and economical to avoid mismatch between water demand and supply patterns, which has a major effect on economic viability of the PVWPS. The study will depart from the traditional methods, which designed and optimized PVWPS components separately and did not account for the dynamics of the head, due to variations of flow rate as influenced by solar radiation. The model optimally sizes the pump, pipe and water storage tank in an integrated fashion, from the climatic data (irradiance and ambient temperature) and the profile of water demand by the users of the system. Thus the method will develop a flow rate to power function from time variations of solar radiation and empirical pump curve data, hence accounting for the dynamics of the flow and head. Therefore predicting hourly flow output, which enable system sizing to be more accurate and economical [17].

1.4 Objectives of the study

Evaluation of parameters that affect the performance of the solar (photovoltaic) water pumping system (PVWPS), for Short and long term planning of solar energy systems requires data on solar irradiation temperatures at the site where the system will be installed, for over large areas; solar radiation maps are essential.

(a) The first objective of this case study is to develop long term average monthly of global horizontal solar radiation, diffuse radiation, maximum and minimum ambient temperature; for the entire area of Lesotho. A computer program that applies the mathematical method of bilinear interpolation is also developed, to enable faster and convenient reading of the mapped solar resource data

(b) To derive power-flow functions that directly relate the PV power to flow rate based on pump manufacturers' empirical pump. To establish hourly response functions as the system reacts to non-linear variations of the flowrate (pump-response) to system resistance as they are functions to solar PV electric output, which is it also the function variable meteorological factors.

(c) Apply Hove and Mungofa model [17] to optimise and size the solar pumping system components using derived power flow functions and long term meteorological data, for hypothetical case study of 350m^3/day potable water supply for Tosing community (-30.36 latitude, 27.90 longitude), Lesotho. The

objective function is to attain the least unit cost of pumping by, sizing the system with combination of optimally sized components.

(d) Apply the developed grid data base of long term monthly averages to predict hourly variations of optimised systems performance, from monthly to hourly time step variations, accurate predictions of water output for Tosing water supply scheme are evaluated. Storage design is accurately sized from this predictions by apply mass balancing approach.

(e) To make recommendations regarding policies for improvement of solar pumping systems development in Lesotho. The implementations of PVPWS require to satisfy from onset; institutional, environmental, social, technical and economic factors to be sustainable in Lesotho.

1.5 The hypothesis of this study

Hypothesis 1: Simple sizing methods of the PVPWS results in oversized system, thus increasing the costs of the system, also the storage designs are oversized with traditional design methods.

Hypothesis 2: The proposed method of optimal sizing and performance prediction of a solar pump-pipe-storage system proposed for this study will result in reduced economic expenses thus improve economic viability of PVWPS and technical efficiency of the system.

1.6 Thesis structure outline

The paper is organized as follows: Chapter 1 is the research introduction; Chapter 2 is the literature review; which presents the principle of PVWPS, solar background, and solar energy assessment, technology advancement an overview of performance analysis research of PVWPS is given and finally explores the design methods of PV water pumping systems. Chapter 3 is the methodology chapter, of applied methods and materials to execute objectives of the study. Chapter 4 presents the results of this study and their discussions. Chapter 5 is the conclusions and recommendations and it is the final chapter of this study.

CHAPTER 2: LITERATURE REVIEW

2.1 SOLAR ENERGY.

2.1.2 Solar energy review.

This type of energy depends on the nuclear fusion power from the core of the sun which produces high temperature and continuous emissions of large amount of energy. Solar energy is emitted to the universe by electromagnetic radiation which is distributed from the infrared to the ultraviolet. Not all radiation reaches the surface of the Earth because shorter ultraviolet waves are absorbed by atmospheric gases primarily by ozone: Approximately one-third of the energy is reflected back. The magnitude that measures the solar radiation that arrives at the Earth is the irradiance (W/m2), which measures the energy that reaches Earth per unit area [18].

Solar energy is a reliable, accessible, free and inexhaustible source of energy, so most of planet has the ability to collect some amount of solar power. According to the European Energy Policies [19], solar energy is non-polluting, does not create greenhouse gases, such as oil based energy does, nor does it create waste that must be stored, such as nuclear energy, neither noise contamination because there are no mechanical pieces in movement. There are two types of solar energy technologies: Solar electric (photovoltaic system) or solar thermal systems.

Photovoltaic energy is obtained directly from the sun and converted into electricity. This kind of technology uses solar cells (PV cells) to convert the sunlight into electricity. A solar cell is made by a semiconductor material (wafer), usually highly pure silicon, consisting of two layers with different properties: One is of n-type and the other is p-type material making a p-n junction. So, when the light radiation from the sun reaches the solar cell, photons hit the semiconductor materials and cause a movement of electrons from the n-type side and to the holes on p-type side of the junction, (Figure 1) [20].

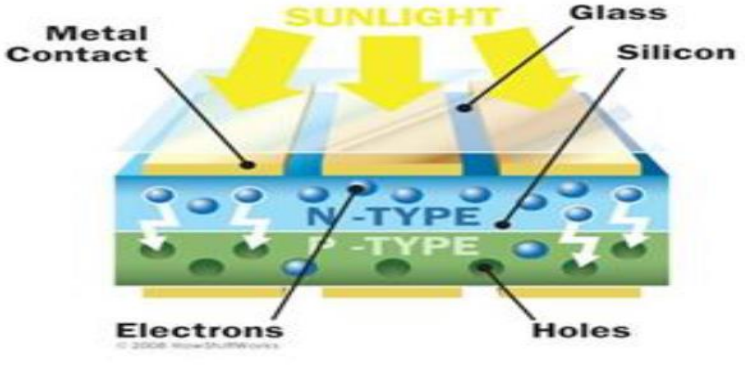

This generates a voltage difference between the front and the back of the cell and a dissipation of power into the load. The voltage produced by a silicon PV cell is around 0,6V. The efficiency of crystalline solar cells is generally 15% under standard test conditions STC [21]. PV cells are connected in series or parallel creating a PV modules, panels or arrays which allows reaching voltage levels commonly used and produce the amount of electricity needed by the load (Figure2)

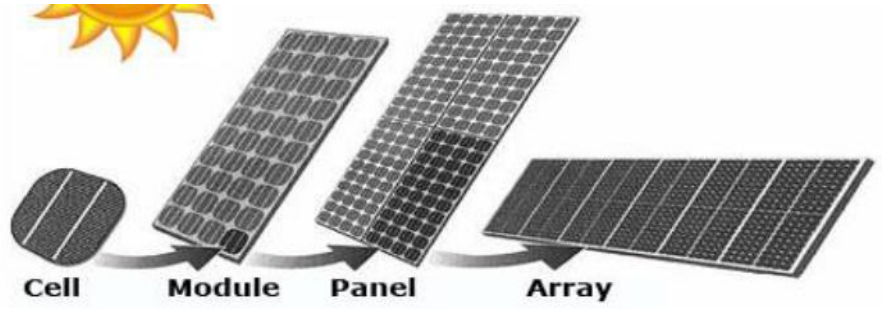

Figure 2 PV cell, module, panel and array illustration. Source: [21]

The cost of new photovoltaic power is dropping rapidly, and if the photovoltaic industry continues to grow and improve technologically, by 2030 the cost will be comparable to the cost of conventional power [21]. Also the installation of photovoltaic systems is quite easy and simple and they have a long life, around 20 years.

2.1.2 Solar energy assessment.

Knowledge of the solar radiation arriving at the surface of the Earth is important for Planning and development of solar energy systems. The basic information required to evaluate the solar radiation available on solar energy collectors of any type, is a measure of the beam and diffuse component of global (total horizontal plane) radiation [21]. Beam radiation is the solar radiation received from the sun without having been scattered by the atmosphere. Diffuse radiation is the solar radiation received from the sun after its direction has been changed by scattering by the atmosphere. Total solar radiation is the sum of the beam and the diffuse solar radiation on a surface. (The most common measurements of solar radiation are total radiation on a horizontal surface, often referred to as global radiation on the surface). Irradiance, (W/m^2) is the rate at which radiant energy is incident on a surface per unit area of surface. The symbol G is used for solar irradiance, with appropriate subscripts for beam, diffuse, or global radiation [22].

Solar radiation shows a strong seasonality in both its average and variability, due to astronomical and atmospheric effects. Solar radiation can be measured using ground sensors or estimated by satellite measures or atmospheric re-analyses [23]. The global radiation ground measurements network in world is still in progress; the average distance between stations is about 100 km even sparser in developing countries and is thus too large for the current applications of solar meteorology. On the other hand, meteorological satellites provide extensive and frequent observations of the earth-atmosphere. The ground resolution depends upon the satellite sensor and the latitude of measurements [24]. In this study, PVGIS: CMSAF (Photovoltaic Geographical information system), (Satellite Application Facility on Climate Monitoring) [25], is proposed to provide data for the period of from 2007 to 2016, of the monthly averages in a regular grid at a resolution of 0:05+ latitude 0:05+ longitude. Then including overall extent of the images is approximately 70_N to 70_S and 70_W to 70_E, characterized by very low overall bias and shows good accuracy at validation sites [26].

For reliable of solar process design and performance evaluation, it is required to calculate the hourly radiation on a tilted surface of a collector to that on a horizontal surface. The most commonly available solar radiation data is in hours or days on a horizontal surface, whereas the need is for beam and diffuse radiation on the plane (tilted) of the collector. The geometric factor R_b, which is the ratio of beam radiation on a tilted surface to that on a horizontal surface: the ratio $\frac{G_{b,T}}{G_b}$. The irradiance incident on the plane of the PV array can be estimated by the simplified tilted plane model justified by Collares-Pereira and Rabl [27].

$$G_T = G_b R_b + G_d \qquad \{\text{eqn.1}\}$$

In equation 1, G_b is the beam component of solar irradiance incident on a horizontal surface, R_b is the ratio of beam radiation on the tilted plane to that on a horizontal plane and G_d is the diffuse irradiance on the horizontal surface. Since instantaneous data of irradiance is not commonly available, it is common practice to use the average irradiance for a one hour period and evaluate R_b at the mid-point of the hour. Even the hourly solar data is rarely available, such that G_T, G_b and G_d have to be evaluated on monthly-average hourly basis.

From the monthly-average daily irradiation on a horizontal plane, $\overline{H}_h$, the monthly-average daily diffuse irradiation, $\overline{H}_d$ is estimated from a diffuse-ratio-clearness-index correlation appropriate for Maseru, Lesotho .The applied correlation model was originally formulated by Hove and Göttsche [28]. Thus adjusted model for Maseru is.

$$\overline{H}_h/\overline{H}_d = -20292_h + \overline{K}_h 1.6118 \qquad \{\text{eqn.2}\}$$

In equation 2, $\bar{K}_h$ is the monthly average clearness index. The monthly-average hourly values for hourly global and diffuse radiation on a horizontal plane, $\bar{G}_h$ and $\bar{G}_d$ are then calculated by use the statistical ratios of hourly to daily radiation, r_h and r_d respectively. The ratios r_h and r_d are functions of sunrise hour angle and sunset hour angle, and their expressions have been given by Collares-Pereira and Rabl [27].

$$r_d = \bar{G}_d / \bar{H}_d = \boldsymbol{\pi} / (\boldsymbol{cos} w - \boldsymbol{co}\text{s } w_s) / (\boldsymbol{s}\text{i}\boldsymbol{n}\ w_s - \boldsymbol{\pi}/\boldsymbol{180} w_s\ \boldsymbol{cos} w_s)$$

$$r_h = \bar{G}_h / \bar{H}_h = (a + b\cos w) r_d \qquad \{\text{eqn.3}\}$$

Where the variables: ω (in radians) is the hour angle and sunset hour angle is ω_s, $a = 0.409 + 0.5016\ sin(w_s - 60)$ and $b = 0.6609 - 0.4767 sin(w_s - 60)$.The models given , enable the determination of the radiation on a tilted surface with only limited data such as the monthly average global horizontal irradiation. Correlation of ground-measured and satellite-measured clearness indices is proposed for the present study. The correlation equation is of the form:

$$\bar{K}_{ground} = b\bar{K}_{satellite} + a \qquad \{\text{eqn.4}\}$$

In Equation (4), $\bar{K}_{\_ground}$ is the monthly clearness index obtained from ground-measured solar radiation data at a station by dividing the monthly average of daily global radiation, $\bar{H}_{\_ground}$, by the monthly average daily extraterrestrial radiation, $\bar{H}_{\_og}$. The value of $\bar{H}_{\_satellite}$ is determined in a similar manner by dividing the monthly average satellite-measured global radiation by $\bar{H}_{\_os}$. The extraterrestrial irradiation over a day can be computed at any latitude on any day of the year. H_o, can be estimated by computing the daily extraterrestrial radiation for the average day of each month, [29]. The coefficients **a** and **b** in Equation 4, **a** is the regression constant in linear equation relating, $\bar{K}_{\_ground}$ and $\bar{K}_{\_satelite}$ **b** is the regression slope coefficient in linear equation$\bar{K}_{_ground}$and $\bar{K}_{\_satelite}$. Although solar radiation is the prominent variable to estimate the power output of a PV plant, air temperature plays an important role too due to its role in the efficiency of the PV panel. To this end, in the analysis the study will use monthly averages of maximum and minimum temperature data.

2.2 SOLAR PV WATER PUMPING SYSTEM (PVWPS)

2.2.1 Evaluation of PVWPS

Maturity of the solar photovoltaic (PV) technology is emphasized by the numerous types of applications encountered nowadays. Photovoltaic water pumping system (PVWPS) is one of the most interesting applications, especially in remote areas where connection to the local grid is not always feasible and the use of fossil fuels is also unsustainable. Some important applications of this technology are for irrigation,

community water supply or hydro-energy storage systems [30]. Figure 3, shows a schematic diagram of a generalized photovoltaic water pumping system (PVWPS). It is composed of a power collection system, power conditioning unit, water pump (submersible or surface), and a water reservoir. The power collection system mostly involves the PV panels that collect solar energy and converts it to electrical energy.

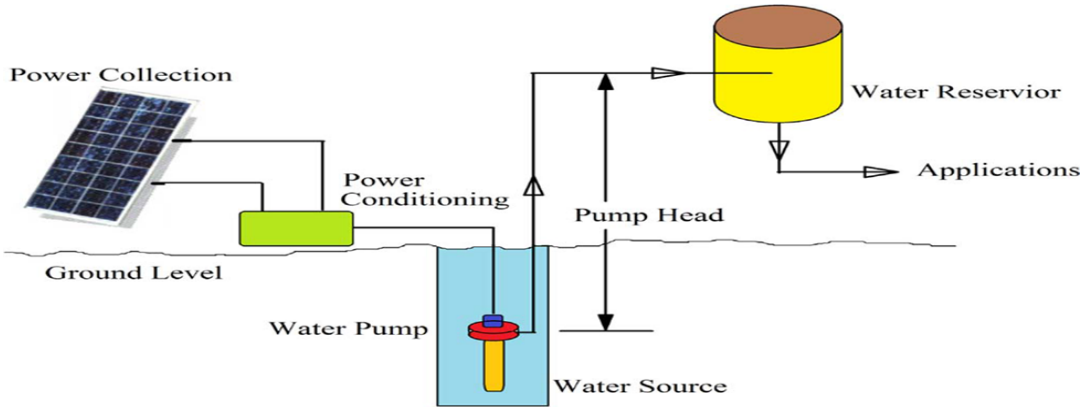

Figure 3 schematic of solar water pumping system source: [31]

The generated electricity is normally DC while most of the water pumps available on the market require an AC electrical input. Therefore, there is a need to condition the generated power from the power collection system so that it can power up the water pump. A water pump is installed in the water source. It pumps the water from the source to a water reservoir located at a higher elevation from the ground level. The elevation difference from the water pump to the inlet of the water reservoir is known as the pump head. This pump head is dynamic and it is an important parameter in designing the pumping system [32].

The design and selection of components of PVWPS require evaluation of parameters necessary for efficient technical performance. PVWPS is application dependent and require specific site conditions to attain sustainability. Campana et al [33], illustrated with figure 4, the necessary parameters to be studied carefully before selection of components and optimal sizing PV system, motor pump-pipe system and storage. Water demand and head profile are basic guiding factors; that determine the motor-pump design load, (the nonlinear load of PV power system). Also The PV electrical output characteristics are nonlinear and vary according to the solar irradiation (G) and the cell temperature (T). The nonlinear operation of this type of system; pose a great challenge in sizing system's components and their selection [32]. Selection of components will depend on application and specific characteristics of the site. There are two types of pumps according to application; submersible or surface water pumps, also their several types of pumps according to the pumping principle.

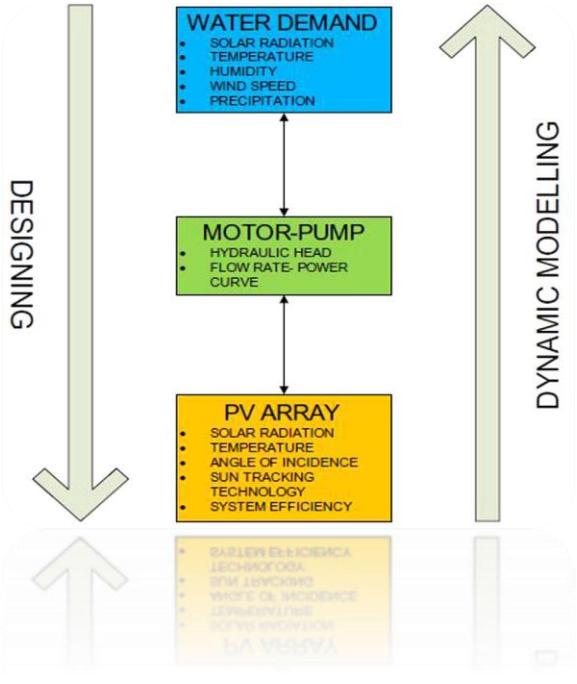

Figure 4 Factors considered for optimal design **Source: [33]**

For the centrifugal pump, the liquid is sucked by the centrifugal force created by the impeller and the casing directs the liquid to the outlet as the impeller rotates. The liquid leaves with a higher velocity and pressure than it had when it entered. The water speed and pressure depend on the available mechanical power at the rotating impeller and the total head. The displacement pump uses a piston or a screw to control the water flow. Screw pumps, where a screw traps the liquid in the suction side of the pump casing and forces it to the outlet. With piston pumps, motion of the piston draws water into a chamber using the inlet valve, and expels it to the outlet using the outlet valve. The positive displacement pump grants a better efficiency under low power conditions than the centrifugal pump [34].

The water pumps may be driven by many types of driving systems. The more popular are direct current (DC) motors, alternative current (AC) motors. In direct-coupled DC systems, operating points deviate considerably from the maximum power point of the PV array at most insolation range [35]. It is unlikely that a direct-coupled system will allow operation at maximum power point of the PV array especially under continuous variation of weather [36]. DC motors have a common disadvantage associated with the sliding brush contacts that require a frequent maintenance. For submersible application, maintaining and replacing brushes need the pump to be removed from the well thus increasing running cost and decreasing reliability. Generally, DC motors suffer from maintenance problem. To overcome this drawback, brushless DC motor were introduced. However, Brushless motors are available for low power applications [37].

A solar energy system should seek to fulfil optimal combination of efficient performance, low initial and running cost, robustness and durability. AC pumping systems using induction motors and invertors offer reliable option. In comparison to DC motors, Induction motors are more rugged, reliable and maintenance free [37]. The range of AC motors available is much greater and its cost is lower. AC systems provide more advantageous for efficiency improvements and control strategies [38]. Some studies [39, 40] reported that: (i) a PV water pumping system driven by an induction motor is attractive for reliability and maintenance-free operation; (ii) Induction motors provide more possibilities of efficiency improvements and diversity of control strategies; and (iii) they have no disadvantage of additional inverter or BLDC motors. Methods for the evaluation of the long term performance of DC, AC, BLDC or induction motors powered by photovoltaic powered are well researched [41].

To establish the utilization of PVWPS systems, the performance evaluation of the PVWPS has been researched vastly. One of the earliest viability assessment programs for PVWPS was initiated by UNDP in1978 in a project given by World Bank [2]. The program known as Global Solar Pumping Project was aimed at determining techno-commercial viability of solar pumps it was found that PV pumping systems were economically viable in countries with high sunshine having high diesel prices and all year round water requirements. Furthermore a lot of research has been focused on increasing the overall technical performance of PVWPS [42].

The most influential parameters on the performance of solar PV systems are: angle of incident, cell temperature, dust accumulation on PV module surface, degradation of PV module. Shadowing, self-shading, and mismatch are complex factors that have a remarkable effect on PVWPS performance. These factors need further investigation, and in all circumstance designers must consider their elimination or limitation [43]. However the main challenge in application of solar water pumping technology is the cost per watt of installed system while meeting load demand. The system design of PVWPS is based on a number of elements, such as the PV array sizing and configuration, motor pump-pipe system sizing, storage tank capacity, and life cycle cost analysis. In fact, a poor sizing of the system's components would affect the system reliability and develop a deficiency [44].

Factors that have so far inhibited the widespread implementation of PVWPS include (i) high initial capital cost, (ii) lack of awareness, (iii) lack of technical installation expertise, (iv) history of failures and (v) lack of sufficient knowledge to predict accurately system daily water output [45], most systems installed have experienced problems, mainly due to poor sizing and lower than expected system output. It was studied that there are clear problems associated with design of PVWPS [46]. Proper sizing of system components is essential for maximum utilization of PV water pumping systems. Improved total system efficiency will reduce the PV array size and thus the capital system cost which is mainly dominated by the PV array cost [47]. Improving the cost effectiveness of PV water pumping systems requires effective utilization of PV energy and

thus oversizing should be avoided. It is also necessary to match the load characteristics with the PV array characteristics [48]. An accurate sizing of such system will contribute in reducing the cost and provides an efficient use of such PVWPS.

A number of researchers [49–52] have established several models to simulate the performance of a PV array. They also developed models to study the performance of the inverter, motor, pump and MPPT. The optimal sizing of PV array and pumping subsystem is the main problem investigated in the research field of solar PVWPS. Yet, there is a challenge of non-linear relationship among the sub systems of PVWPS, requiring numerical skills to deal with the models. The models proposed do not show a direct relationship between the operating electrical power of the pumping subsystem and the water flow rate of the pump-pipe and the storage sizing. However, most of the models are based on the characteristics of separate components that are available from the manufacturer empirical data. These models also ignore the variations caused on the system by solar source variations. These models do not holistically size the system components as unit system, in addition the available methods are based on a specific pump and motor for a specific site. So, these methods are difficult to be used in different locations and systems. [53].

Traditional way of selecting the pump is based on maximizing the efficiency of pump at single duty point at a certain one operating flow rate, which is not useful for PVWPS working at a variable flow rate [54]. The proposed method starts by considering the pumps with H-Q (head - flow rate) curves with variable water flow into the storage tank; this variability depends on the instantaneous PV-power available. The higher this PV power, the higher the speed of pump and consequently increased water flow. This is the main difference with the conventional systems supplied by the grid or diesel generators that usually work in the same duty point, providing constant water flow [55]. However, this simple traditional way of selecting is not valid for PVWPS because they work at different flow rates and therefore at different operating points.

For the design of technically and economically optimum PVWPS, estimates of long-term system performance are required. Researchers [53, 56] have; established models for system optimisation. Also prediction models were established [15]. The proposed Hove and Mungofa model [17], pose advantage of being more holistic, accurate and economical in terms of sizing and prediction. Different techniques can be used for optimal sizing; intuitive, analytical, numerical or intelligent. The intuitive methods are based on the designer's experience, and in this method, simple mathematical equations are used and the estimation is usually oversized. The numerical and analytical methods are simple and more accurate, with the support of empirical relationships to calculate the sizing of the components of PVWPS [57].

The numerical methods use simulation- based programs for calculating size according to the time interval, usually hourly, considering different parameters. Generally the most used software are PVSYST [58], HOMER [59], Retscreen [60], SAM [61], MATLAB [62], TRANSYS [63], LABVIEW [64] and others; which can compute

system performance with a high temporal resolution and integrate the results over time. The use of such computer software, however, requires a significant amount of expertise and financial resources. Also, the high resolution meteorological data required by simulations are normally not available for extended periods at many meteorological stations [65].

For functioning of this software models, mathematical equations describing the system characteristics are formulated and implemented into computer codes to be used in the simulation process of the software [66]. Yet these software models do not comprehensively optimize, -the solar PV array, pump-pipe and storage while considering cost unit system of pumping, non-linear time – step variation of climate, water demand profile and other specific characteristic of the location. They neglect some important variables; technical and /or socio-economic parameters, which are decisive for sustainable designs and application of this technology [57], hence they cannot fulfil the objectives of this study.

Similar numerical and analytical techniques are combined and applied in this paper, however another approach is to use simplified computational methods which are adaptable to hand-calculation of mathematical equations governing, the whole system , with simplicity and reduced cost. Hand-calculation methods also give a more intuitive understanding of the subject matter under consideration than do computer software methods. Hove emphasized [65] the advantage of using simple methods suitable for hand calculations but with the calculation speed is enhanced by use of spreadsheets. For this study application Microsoft Excel [66] is applied. Excel is a good utility program for data recording, calculations, plotting, and is actually used a lot by practicing engineers in industry. The main reason for its popularity is simply cost and convenience (most people have it on their computers) making information sharing very easy [67].

Khatib et al. [68] when analysing different size optimization techniques for PV systems, concluded that simulation based on mathematical (numerical and analytical) modelling methods are most widely used techniques and are more accurate. However there are intelligent methods which apply artificial intelligence techniques such as artificial neural network, genetic algorithm, fuzzy logic etc. to solve complicated optimization problems [57]. Concerning intelligent methods, Loxsom & Durongkaveroj [69], demonstrated this methods. Furthermore, intelligent methods are highly accurate and reliable for sizing optimization but very complex to implement

Hove and Mungofa model, adapted for this study applies Microsoft Excel, to simulate results for sizing a solar, pump-pipe, water storage at the least cost of pumping, for optimal design. The model was originally demonstrated in the study of Hove and Mungofa [17], for Binga location in Zimbabwe. The selected model is suitable for PV water pumping applications at a variable speed that is based on considering not only the efficiency at the maximum operating point but in the whole range of operating points [37]. This dynamic

method also considers the selection and sizing of system's components, which operates in wide range of operating frequencies, for least cost of pumping and optimal efficiency.

The mentioned method for optimal sizing and performance prediction of a solar pump-pipe-storage system is proposed in this study, for climate and socio-economic conditions of Lesotho. The solar-pumping-system components namely, the pump; solar photovoltaic array; piping system and the water storage, are sized in collective strategy. The method formulates a flow-power function, from manufacture's empirical data of the system components, and takes into account the time-step variation of solar irradiance and its effect on the pump system flow-rate and total dynamic head. The flow-power function specify the flow output of the solar pumping system as a function of the time-step variation of the photovoltaic array power output, for a given pump and pipe size[17].

From the factory gate to site of installation the relative specific costs of PV array, pump and pipe differ from place to place, an economically optimum combination of these sub system components, which meet the required daily demand of water at the least cost of pumping, can be attained [17]. Applying a time-step balance of the hourly pump flow output with the hourly water demand also enables a more exact estimation of the required balancing storage, through the mass-balance-curve approach

2.3. Optimisation of PVWPS

2.3.1Hydraulic power- flow function modelling.

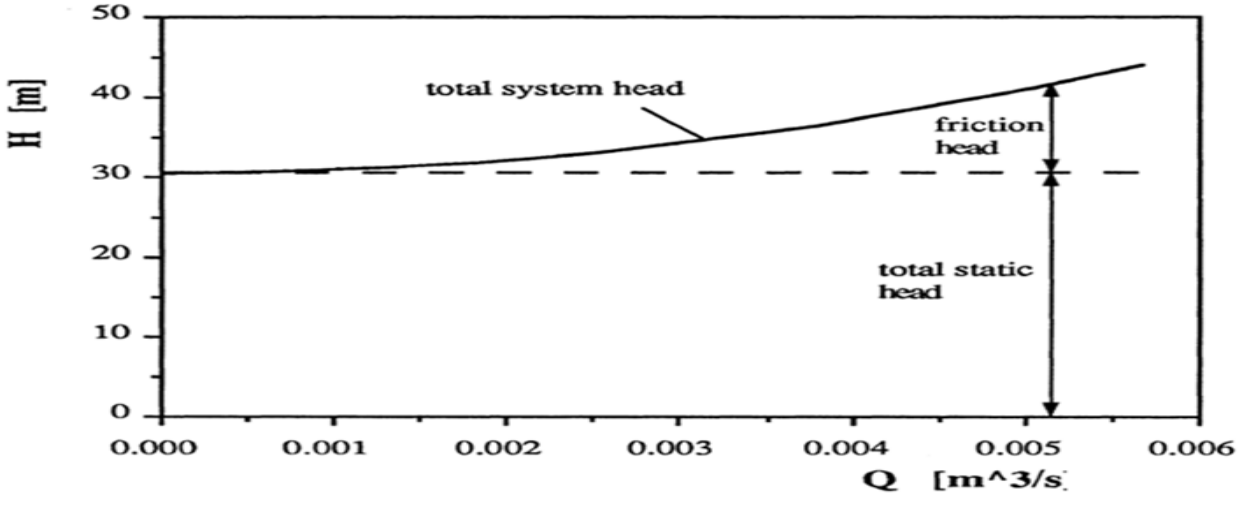

Figure 5 Typical illustration of head profile Source: [42].

A typical head profile for PVPWPS is shown in Figure 5; the total static head is defined as the difference in height between the water supply surface and the water discharge level. The friction head is the needed pressure difference specified in meter liquid to overcome the friction caused in the piping system. The

friction head is a function of flow-rate. First the pump system is analysed and a system head-flow rate (H-Q) relation is derived [42]. The equations describing the pump are developed using correlations from pump manufacturer data and fundamental pump relationships. The objective is to find the flow- rate / power relation function. The performance of pump system is commonly visualized as head versus flow-capacity characteristics. For sampling the performance curves are shown in Figure 6; as provided by a pump manufacturer [70].

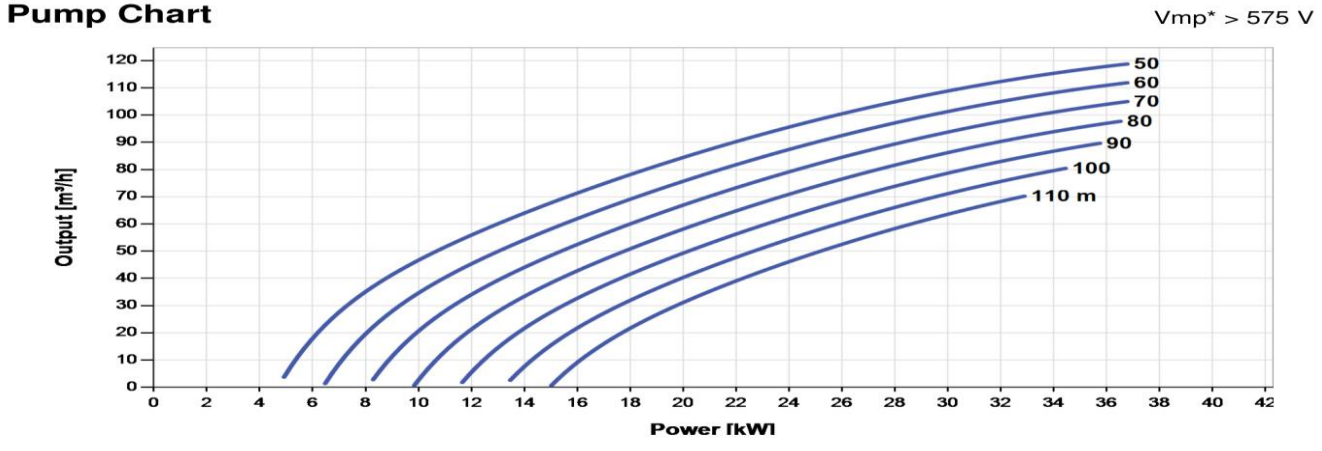

Figure 6 lorentz PSk-2-40-C-SJ95-7 pump curves. Source[70]

In the analysis and design of pumping systems, it is useful to superimpose the system characteristics on the pump characteristics as shown in Figure 7. The operating points are the intersections of the system curve and the pump curves [42]. When a pump is started, first it operates along the head axis at zero flow rate until the system static head is reached. Then the flow starts and the actual operating points depends on the speed of the pump. For PV powered water pumping systems operation over the entire pump speed range is possible. To find the operating points of a pump, it is necessary to condense the pump performance data, provided by the manufacturer, into a useful equation [42].

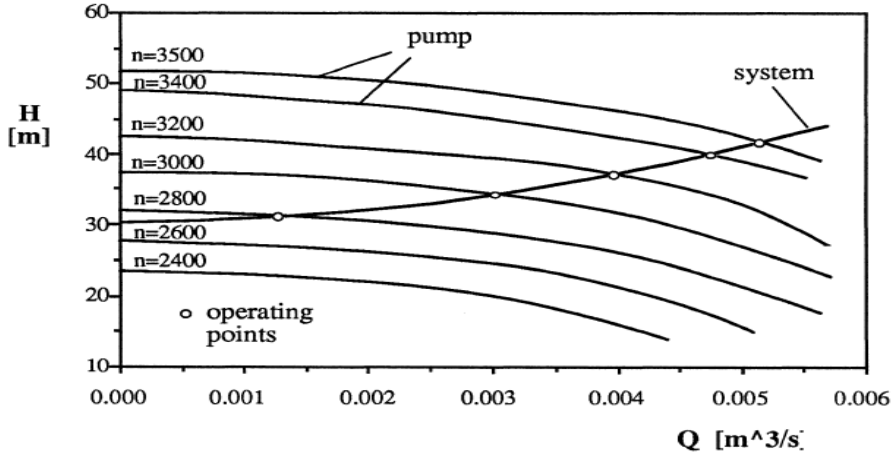

Figure 7 Superposition of system's curve and pump curves

Fundamental pump laws supply the additional relationships required to obtain the pump speed-power characteristics, the head profiles are geometrically similar. This means that if the performance curve for one speed is known, it can be obtained for other speeds by moving the curve up or down [42]. The curves are theoretically moved along a parabola with the head axis as the main axis. Further, following the *affinity laws* [71], which relate speed to flow-rate, head and power, are obeyed. The premise of the first set of affinity laws is that: For a given pump with a fixed diameter impeller, the capacity will be directly proportional to the speed, the head will be directly proportional to the square of the speed, and the required power will be directly proportional to the cube of the speed.

Hove and Mungofa observed that, as the PV power supply level (voltage) varies, the speed of the solar pump varies as well. Therefore, as many head-flow (H-Q) pump curves as there are levels of power supply can be defined. For each selected PV power supply level on Figure 6, a pump H-Q curve can be obtained by reading corresponding pairs of H and Q values and then fitting a best-fit curve relating H and Q. The H-Q relationship is of the form [17]:

$$\mathrm{H} = \mathrm{p}_2 Q^2 + \mathrm{p}_1 Q + \mathrm{p}_0 \qquad \{\text{eqn.5}\}$$

From equation 5, H [m] is the pump head at a flow rate Q [m3/hr], p_0, p_1, and p_2 are the pump-specific regression coefficients given by empirical results. The flow rate Q increases with the increase of pump power for different heads following the nonlinear model as indicated in the relation. The pump, by itself, does not create pressure. Pressure results only when there is resistance to flow. It cannot have pressure without flow (or potential flow). p_0, p_1, and p_2 are the parameters of the pump model and depend only on the pumping subsystem [12].Accounting for the head-profile; static head H_0 and H_L, frictional loses (resistance) are considered and minor abrupt losses are neglected for long pipe line. Thus the total dynamic head is defined as [17]:

$$\mathrm{TDH} = \mathrm{H}_0 + \mathrm{H}_\mathrm{L} \qquad \{\text{eqn6}\}$$

Resistance can be calculated for each flow rate using the Hazen-Williams formula [72], an empirical equation which relates the flow of water in closed conduit. The equation pre supposes a fluid has kinematic viscosity of 1.13 centistokes with turbulent flow. Water viscosity fluctuates with temperatures, the proposed method is simple and reliable at temperatures around 2˚C to 25˚C. Hazen-William equation is popular to analyse typical water supply systems and it is not suitable for other fluids and is given as:

$$V = 0.85 C \left(\frac{D}{4}\right)^{0.63} S^{0.54} \qquad \{\text{eqn.7}\}$$

Where V [m/s], is the flow velocity, D[m]is the pipe diameter of the pumping main, Q [m3/s] is the volumetric flow rate, C is the Hazen-Williams coefficient and S is the slope (h_l /L) ratio of frictional loss to the length of the pipelines).

The system's curves will vary accordingly for different pipe diameters, producing system curves for each pipe diameter sampled. The premise of the second set of *affinity laws* [71] is obeyed: For a given pump with a constant speed, the capacity will be directly proportional to the impeller diameter, the head will be directly proportional to the square of the impeller diameter, and the required power will be directly proportional to the cube of the impeller diameter. The total dynamic head *T*DH can be expressed in quadratic equation of the form [17]:

$$TDH = H_0 + h_1 Q + h_2 Q^2 \quad \{eqn.8\}$$

Parameters h_1 and h_2 are system coefficients, and are analysed from system curve. The intersection of the *Hpump* and TDH curves defines the operating flow rate Q_{op} and operating head TDH_{op} for the pump when connected to the respective pipe line diameters of the previously specified length. Q_{op} and TDH_{op} can be read from Figure 7 or they may be obtained analytically as the simultaneous solution of equation 5 and equation 8 therefore [17]:

$$Q_{op} = \text{MAX}[0, \frac{(h1-p1)\sqrt{(b1-h1)^2-4(p2-h2)(p0-H0)}}{2(p2-h2)}] \quad \{eqn.9\}$$

$$TDH_{op} = H_0 + h_1 Q_{op} + h_2 Q_{op} \quad \{eqn.10\}$$

From equation 9 and equation 10, TDH_{op} is the total dynamic head at operating point and Q_{op} is the operating flow rate. Finally, the operating flow rate Q_{op} is correlated with the speed (n) in revolutions per minute as a function of P_{pv} read from Figure 7, by pairing each Q_{op} with the corresponding P_{pv},. The $P_{pv}-Q_{op}$ correlation function is logarithmic and parametric with pipe diameter [17]; and it is of the form:

$$Q_{op} = q1 \ln(P_{pv}) - qo \qquad for\ P_{pv} \geq P_{off}$$

$$Q_{op} = 0 \qquad for\ P_{pv} < P_{off} \quad \{eqn.11\}$$

In equation 11, P_{off} is the minimum PV power which can make the pump start running. Subsequently, the electrical to hydraulic operation efficiency of the solar pumping system for each PV power (a function of collected solar radiation, PV solar-electricity conversion efficiency and PV array size) is obtained as in equation 12[17]:

$$\eta_{pump} = \frac{\rho g Q_{op} TDH_{pv}}{P_{pv}} \quad \{eqn.12\}$$

2.3.2 PV power out modelling

As demonstrated in the past section, the solar pump performance output Q_{op}, TDH_{op} and $\eta_{pump\text{-}op}$ are by the PV power output P_{pv}. Also, P_{pv} is dependent on the radiation collected on the plane of the PV array, the PV

module's solar-electric conversion efficiency and its size and rated efficiency. The photovoltaic power is defined as by Hove 2018 PV model [17], based on efficiencies of the system, unlike Hove 2000[65], which its analytic objective is in terms of area.

$$P_{pv} = \frac{\eta PV}{\eta STC} * \frac{Gpv}{G\,sTc} * P_{STC} \qquad \{eqn.13\}$$

From equation 13, P_{STC} [Watts] is the rated power of the PV Array at Standard Test Conditions (STC), η_{STC} is the operating efficiency, G_T represents the irradiance measured on a tilted plane and G_{STC} is the reference irradiance. The PV efficiency is a function of temperature and is related to other constants by equation 14 [17].

$$\eta_{pv} = F_M\,[1-\beta(T_{CELL}-25)]\,\eta_{STC} \qquad \{eqn.14\}$$

In equation 14, Fm is the matching factor described as a ratio of power output of the PV array under varying operating conditions to its power output at maximum power point. A value of 0.9 is general accepted in PV system [53], the other parameters are β (cell efficiency temperature coefficient), and T_{cell} (cell temperature), are usually given on manufactures product data sheet. Since cell temperature is difficult to monitor under field operation, it is convenient to correlate it with, the ambient temperature, T_a. The standard equation for relating PV cell temperature with ambient and in-plane solar irradiance, which neglect the effect of wind speed on cell temperature, is given by

$$T_{CELL} = T_a + \frac{GT}{GsTC}(T_{C,\,NOCT} - T_{a,\,NOCT}) \qquad \{eqn.15\}$$

From equation 15, $T_{c,\,NOCT}$ [°C] is the nominal operating cell temperature (NOCT), $T_{a,\,NOCT}$ ambient temperature at NOCT and, $G_{T,\,NOCT}$ is the irradiance at NOCT. The average PV array efficiency $\bar{\eta}_{pv}$ is obtained as the total summation of the hourly PV power over the day divided by the sum of hourly irradiance multiplied by the PV array area. Also the average pump efficiency $\bar{\eta}_{pump\_op}$ is the sum of the hydraulic power output $\Sigma\rho g Q_{op} TDH_{op}$ divided by ΣP_{pv}. The overall electric-to-hydraulic efficiency $\bar{\eta}_{total}$ is then $\bar{\eta}_{pv} \times \bar{\eta}_{pump\_op}$.

2.3.3 Economic model

The technical factors are related to the (PVWPS) system performance, PV power, components efficiencies, electrical power, TDH, and others. Yet, an economic evaluation of solar water pumping systems is based on the monetary values of the system. The most used methods are; Net Present Cost (NPC), Life Cycle Cost (LCC), Levelised Cost of Electricity (LCOE), Internal Rate of Return (IRR) and Benefit-to-Cost Ratio (BCR).

In this study an appropriate objective-function metric to use for comparison is the unit cost of pumping, based on Life Cycle Cost analysis method. Life cycle cost (LCC) analysis, is considered the most widely used method for evaluating the cost of a desired system [66]. Life cycle cost analysis gives the total cost of the PV

powered water pumping system including all expenses incurred over the life of the system, and it is helpful for comparing the costs of different system designs. The unit cost of pumping is calculated as the annualized cost of the sum of capital costs (C_{CAPEX}) of the solar PV array; the pump-pipe system and the pump-motor-conditioning unit, plus the annual maintenance costs (C_{OM}), all divided by the annual volume of water pumped. For each capital asset of the pumping system, the annualized cost is calculated from euation.15, for a discount rate of $r\%$ and an asset life of n years [17].

$$C_{COST\ OF\ PUMPING} = C_{CAPEX} \times \frac{r}{1-(1+r)\hat{}-n} + C_{OM} \quad \{eqn.16\}$$

2.3.4 Storage tank model

As research gap, it is possible to understand from different authors that the design methodologies used do not explore the dynamic nature of the end-use of PVWPS. Models that are close to the practical reality of user's can contribute positively to the massive adoption of technology.[57] The fundamental goal of a solar-powered water pump system is to store water, not electricity. The use of batteries should therefore be avoided unless absolutely necessary since the added expense and complexity usually outweighs any advantages. Water storage is suitable for this application of solar water pumps.

The conventional water supply systems are designed to contain (2 to 5 outages) dark days multiplied by the average daily water demand. This method of sizing usually leads to problems, especially for fluctuating demand and fluctuating supply of water. The minimum tank sizing is estimated by simulating long term daily weather data, thus estimating the water balance from daily water demand and production. In this studied the quantity of water required to be stored in the reservoir for equalising or balancing fluctuating demand against fluctuating (balancing storage) can be worked out by mass curve method. The method applies the principle of water balance which is the difference between daily water production and water demand: That for poor consecutive days of solar radiation, from those days with maximum requirement of water demand is exactly the maximum deficit and from the cumulatively surplus the balance of storage can be analysed [17, 68]. Water tank size, required to fulfill any user's need, is analysed from the daily water demand profile of the user, it therefore essential for this procedure.

CHAPTER 3: METHODOLOGY

3.1 Description of the applied model.

The Applied Hove and Mungofa method of optimal sizing and performance prediction of solar PV-pump-pipe and storage system is quantitative research method and it is demonstrated in this present study. The optimisation, efforts are mainly focused on minimizing the cost and improving the efficiency of the system. Prediction of the dynamic performance of PVWPS is important for the designer and the user of such system [73]. The applied method sizes system's components (solar PV-pump-pipe and storage system) in integrated fashion. With attributes of proper matching and sizing of PVWPS system's components this method yields improved optimal efficiency of a system. Again with different combinations of properly sized components of the system, the least cost of pumping can be attained [17].

For the purpose of demonstrating the processes of this model and analyse the results of Lesotho's operating conditions. The hypothetical case-study solar powered pump-pipe system, whose site preliminary information is given on Table 1, is studied.

Table 1 Preliminary site information

Item	Description
Location	Tosing, Quthing-Lesotho -30.36 Latitude, 27.90Longitude
Average daily water demand	350[m^3/day]
Static head	60m (40m well depth at upper aquifer level +10m pump immersion distance +10m from surface to water to tank)
Pumping distance	3000m
Pumping mains	M-PVC Modified poly vinyl chloride 125mm,140mm,160mm,177mm,200mm
Pump type	**(To be selected)**
Water demand application /water source	Rural community water supply (Potable water supply)/ borehole well

The Hove and Mungofa model for optimisation of solar PV pump-pipe and storage system is adapted by Hove who developed Microsoft Excel based computer simulation program to evaluate the model. This approach is adopted in this study, together with to be developed interpolation program the model ability to read meteorological data (solar radiation and ambient temperature) over Lesotho, developed for this study. The relevant parameters are inputted into the simulation program of solar_pump_pipe sizing, of user face of the program as captured and shown by table 2.

Table 2 User face of simulation program (illustrating design inputs)

COMPUTER PROGRAM INPUTS		
INPUT	VALUE	UNIT
MONTH	Jun-00	
Average date	11/06/2019	
LONGITUDE	27.90	°(Degrees)
LATITUDE	-30.36	°(Degrees)
AZIMUTH	180	°(Degrees)
TILT	35.36	°(Degrees)
$T_{a\ max}$	12.5	°C
$T_{a\ min}$	-1.03	°C
GHI	11.83	MJ/m^2
	3.29	KWh/m^2
PV module parameters		
ηSTC	16%	
β	0.0041	/oC
fm	0.9	
NOCT	46	oC
PV POWER	20277	Watts
System Resistance Curve		
Static head, Ho	60	m
h1	0.025	
h2	0.002	
Flow-power function		
q	33.38	
q0	-35.56	

The proposed method is based on developing a flow-power function from the manufacture's empirically tested system's components data, which are able to more accurately account for time-step response of pump flow output to variation of meteorological conditions at a given site, than some previously reviewed performance prediction models [74,75.]

To apply this method the following sequential steps are performed to establish design data for optimization of PVWPS in this present study.

- Mapping and automation long term metrological parameters by developing grid data base and constructing a bilinear interpolation program specifically for Lesotho.

- Optimal sizing of PVPWS performed by initially by evaluating the design month from the long term meteorological variables.
- System components sizing and deriving Flow-Power Functions: (i) Solar pump selection and deriving iso-power Head-Flow (H-Q) pump curves. (ii) Pipe system selection and sizing and evaluation of system resistance. (iii) Sizing and configuration solar PV array and deriving the operation flow-head-power functions of the PV pump.
- Evaluating cost of pumping for the comparison metric of *unit cost of pumping.*
- Storage sizing from hourly variations of the required water supply and the demand hourly.

3.2 Mapping and automation of metrological parameters.

Accurate and detailed knowledge of spatial and temporal distribution of solar radiation and ambient temperatures of a specified location, are primary requirements for optimal sizing and performance predictions of solar energy systems. For large scale regions such as this present study case, where Lesotho is the specified region, accurate and maximum energy output of sustainable solar energy systems should be based on exact calculations, because energy output is influenced by different factors, such as local climatic conditions (solar radiation availability in different seasons, local cloudiness or fogginess in winter, temperature and so on [76, 77].

From onset the first objective of this study is to develop the global radiation, diffuse radiation, maximum and minimum temperatures grid data base. Grid data ranges from the satellite-derived values at 0.25 ×0.25 longitude and latitude interval for the range 27.00 East to 30.00 East and 28.00 South to 31.00 South. The range defines the extreme longitude and latitude boundaries of Lesotho. For application of this grid data base, it is integrated into the proposed computer model. Since the data is in gridded format bilinear interpolation technique is applied, to estimate magnitude of this meteorological variables at any point in between the grid points.

Implemented with this Lesotho meteorological data, Hove model when inputted of any coordinates in Lesotho it automatically shows interpolated values of radiation and temperatures, as illustrated in table 3. To visualize grid data base in a map form and validate applied bilinear interpolation, accredited Surfer software is used. Surfer is a grid-based mapping program that interpolates irregularly spaced XYZ data into a regularly spaced grid [67]. The process of developing, interpolating grid data base and implementing it into computer model is described in the following subsections.

3.2.1 Developing solar radiation grid data base.

Ground radiation measurements network in developing countries is still in progress, the average distance between stations is above 100km [24], thus is too large for the current applications of solar meteorology. Solar surface irradiance derived from geostationary satellite measurements is usually more accurate than that interpolated from the ground-based measurements which are more than 30 km apart; [79].

A number of solar radiation databases sources are available, some for free, while others are commercial products. See Suri et al. [80] for an inter-comparison of some products. Information on solar radiation and related parameters is also available on the Internet; for comparison see the websites Soda [81] (http://www.soda-is.com), Satel-Light [82]-(http://www.satellight.org), (http://eosweb.larc.nasa.gov/sse) NASA-SSE [83] and NREL [84] http://rredc.nrel.gov/solar. Although these sources provide data with global or continental coverage, their spatial resolution is relatively coarse $1° \times 1°$ for the NASA, 40×40 km for the data from NREL.

This coarse spatial resolution can lead to anomalous predictions, particularly in mountainous regions where data accuracy is lower. To account for spatial variations of solar radiation in areas with dynamic terrain, solar radiation models integrated within geographical information systems (GIS) are helpful. Solar radiation models incorporate physically based and empirical equations to provide rapid and accurate estimates of radiation over large regions, while also considering surface inclination, orientation and shadowing effects [26]. PVGIS-CMSAF [85];(available online at http://re.jrc.ec.europa.eu/pvgis.); for its advantage of coupling radiation models with GIS is applied in this to retrieve average monthly global and diffuse solar radiation of the period 2007-2016, for this study. Also it has large coverage that extent to regions such as Lesotho, with overall extent of the images approximately 70_N to 70_S and 70_W to 70_E and is characterized by very low overall bias and shows good accuracy at validation sites [26].

Type of solar radiation data selected for the current application, is the inter-annual single point data, in average monthly form. Both global and the ratio of diffuse radiation over global radiation data was downloaded from PVGIS-CMSAF website, in a spreadsheets format. The monthly average diffuse component of radiation can be evaluated from the global radiation by the use of an appropriate empirical correlation relating the monthly average diffuse fraction to monthly average clearness index as shown in equation 2.

Typical meteorological year data (TMY) was avoided in this study, even thou it is in useable hourly form. The reason; is that TMY data contains numerous parameters; that are not relevant for the current application. The average monthly data is analysed firstly by averaging each month for the period of 2007-2016.

The resultant is the long term monthly averages of both global and diffuse radiation on horizontal plane and they are implemented into the computer program as shown in table 3. The model assumes that all radiation in an hour is assumed to be concentrated at the middle of the hour, and then it gives the hourly irradiation incident on the tilted plane, with angle of incident measured at the middle of the hour. The applied model is able distribute monthly radiation data to shorter periods of hourly intervals using equation 8 and 9, also Klein[29] average day of the month is applied, illustrated by table 4.

Table 3 Example of global horizontal irradiation grid data base

LONGITUD	*LATITUTDI*	Jan-00	Feb-00	Mar-00	Apr-00	May-00	Jun-00	Jul-00	Aug-00	Sep-00	Oct-00	Nov-00	Dec-00	*ANNUAL*
27	-28	7.11	6.99	5.88	5.00	4.21	3.77	4.15	5.12	6.22	6.90	7.33	7.38	**4.93**
27.25	-28	7.15	6.96	5.88	4.95	4.23	3.77	4.17	5.14	6.22	6.88	7.35	7.45	**4.96**
27.5	-28	7.06	6.85	5.76	4.90	4.22	3.77	4.16	5.14	6.19	6.81	7.27	7.35	**4.93**
27.75	-28	6.87	6.73	5.76	4.83	4.18	3.74	4.14	5.09	6.13	6.70	7.10	7.23	**4.87**
28	-28	6.73	6.76	5.65	4.79	4.15	3.71	4.14	5.06	6.07	6.59	6.98	7.13	**4.84**
28.25	-28	6.78	6.76	5.65	4.74	4.16	3.73	4.13	5.03	6.00	6.49	6.87	7.06	**4.83**
28.5	-28	6.71	6.75	5.61	4.78	4.17	3.75	4.13	5.03	5.98	6.40	6.83	7.02	**4.83**
28.75	-28	6.69	6.75	5.62	4.75	4.14	3.77	4.10	5.00	5.96	6.34	6.73	6.94	**4.82**
29	-28	6.74	6.78	5.66	4.79	4.18	3.78	4.12	5.02	5.95	6.32	6.77	6.98	**4.86**
29.25	-28	6.56	6.70	5.62	4.75	4.15	3.75	4.07	4.97	5.93	6.25	6.69	6.92	**4.83**
29.5	-28	6.47	6.66	5.50	4.74	4.16	3.76	4.10	4.94	5.88	6.16	6.61	6.73	**4.80**
29.75	-28	6.35	6.49	5.37	4.63	4.07	3.68	3.99	4.83	5.57	5.72	6.25	6.59	**4.66**
30	-28	6.49	6.73	5.55	4.73	4.09	3.71	3.98	4.89	5.58	5.89	6.44	6.83	**4.78**
27	-28.25	7.18	6.95	5.86	4.89	4.17	3.74	4.12	5.10	6.18	6.89	7.40	7.49	**4.91**
27.25	-28.25	7.19	6.97	5.92	4.97	4.22	3.76	4.14	5.14	6.22	6.96	7.47	7.55	**4.96**
27.5	-28.25	7.03	6.85	5.84	4.91	4.18	3.73	4.13	5.11	6.18	6.83	7.38	7.43	**4.92**

Table 4 Klein's average day of the month **Source [29]**

Month	**Jan**	**Feb**	**Mar**	**Apr**	**May**	**Jun**	**Jul**	**Aug**	**Sept**	**Oct**	**Nov**	**Dec**
Average day	17th	16th	16th	15th	15th	11th	17th	16th	15th	15th	14th	10th

Interpolation is the process of estimating the values of the points in areas where no original data points exist [67]. There are several interpolation techniques such as kriging, polynomial regression, and natural neighbor and so on, applied according to problem at hand. To interpolate 0.25 longitude ×0.25 interval latitude grid data for this study, bilinear interpolation technique is suitable. From mathematics, bilinear is an extension of

linear interpolation, for Interpolating functions of two variables, for example on two dimensional (2D) grids [86], as illustrated by figure 8. Suppose that we want to find the value of the unknown function f at the point (x, y) at point **P**. It is assumed that we know the value of $f(x, y)$ at the four points $Q_{11} = (x_1, y_1)$, $Q_{12} = (x_1, y_2)$, $Q_{21} = (x_2, y_1)$, and $Q_{22} = (x_2, y_2)$.

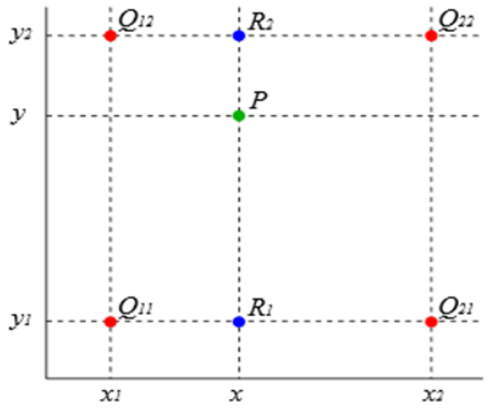

Figure 8 2Dimensional Interpolation problem **Source [12]**

The way to write a solution to this type of the interpolation problem is to interpret 2D grid in a form of a matrix [87], as shown by equation 14. Thus the solution to values at point P is obtained by solving equation 15.

$$\begin{bmatrix} 1 & x_1 & y_1 & x_1 y_1 \\ 1 & x_1 & y_2 & x_1 y_2 \\ 1 & x_2 & y_1 & x_2 y_1 \\ 1 & x_2 & y_2 & x_2 y_2 \end{bmatrix} \quad \{eqn14\}$$

$$f(x, y) \approx b11 f(Q11) + b12 f(Q12) + b21 f(Q21) + b22 f(Q22) \quad \{eqn15\}$$

The coefficients of matrix ($b11$, $b12$, $b21$, $b22$) are determined by solving the following algorithm of a linear system.

$$\begin{bmatrix} b_{11} \\ b_{12} \\ b_{21} \\ b_{22} \end{bmatrix} = \left(\begin{bmatrix} 1 & x_1 & y_1 & x_1 y_1 \\ 1 & x_1 & y_2 & x_1 y_2 \\ 1 & x_2 & y_1 & x_2 y_1 \\ 1 & x_2 & y_2 & x_2 y_2 \end{bmatrix}^{-1} \right)^{\mathrm{T}} \begin{bmatrix} 1 \\ x \\ y \\ xy \end{bmatrix} \quad \{eqn16\}$$

From equation 15 if known values x and y represent longitude and latitude respectively of unknown radiation (Q_{XY}) at point **P**, then known radiations at the four corner points (Q_{11}, Q_{12}, Q_{21}, Q_{22}) of 2D grid with known grid coordinates (x_1, x_2, y_1, y_2) at the respective corners of 2D grid, are used to obtain radiation Q_X from equation 15 and 16.

To apply this bilinear interpolation algorithm for this study it needs to be encrypted into computer program for automatic, faster and numerous interpolations of estimating radiation at any location in Lesotho. To perform the construction of interpolation program; Microsoft Excel spreadsheets [67] are utilized. From table 2, gridded solar radiation data is **xyz** format, where **x** denotes Longitude, **y** denotes Latitude and **z** is any month of the year. The month to analyse **z** is selected together with appropriate average day on the computer program inputs.

To determine the bilinear interpolation matrix of **x** and **y** longitude and latitude, for the spreadsheet program, firstly the coordinates of case study are the inputted. The **ROUNDUP** and **ROUND DOWN** functions of spreadsheets are applied on **x** and **y** coordinates, to determine the known grid coordinates **(x_1, x_2, y_1, y_2).** Furthermore the **IF** function of series of interval of (1, 0.75, 0.5, 0.25, and 0) is programmed to match with the grid data intervals to locate the known grid coordinates. **INDEX** and **MATCH** functions are used find appropriate solar radiation values **(Q_{11}, Q_{12}, Q_{21}, Q_{22})** from the gridded radiation and their respective coordinates **(x_1, x_2, y_1, y_2)**. From table 5 the inverse matrix was delivered by application of **MINVERSE** on interpolation matrix and coefficients of bilinear interpolation matrix were obtained by **MMULT** function, multiplies the inverse matrix with solar radiation values (Q_{11}, Q_{12}, Q_{21}, Q_{22}). Equation 15 is implemented into the model to estimate the radiation of inputted coordinates, table 4 shows interpolated data $f(x, y)$ in mega Joules units.

Table 5 Illustration of global horizontal radiation interpolation program

interpolation matrix												
1	27.75	-30.25	-839.44			11.3352						
1	27.75	-30.00	-832.5			9.7						
1	28.00	-30.25	-847			11.7						
1	28.00	-30.00	-840			11.8						
INVERSE MATRIX							**COEFFICIENT MATRIX**			**LONGITUDE/LATITUDE**		
	-13440	13552	13320	-13431			-23165			x	27.90	
	480	-484	-480	484			827.976			y	-30.36	
	-448	448	444	-444			-764.77					
	16	-16	-16	16			27.3216					
	INTERPOLATED DATA											
	f(x,y)	11.8										

2.2 Developing temperature grid data base.

Temperature data used in this study was retrieved from NASA SSE [83]; Available online at https://power,larc.nasa.gov/data. For reliable energy systems that are predictable. Satellite data was chosen for this study for its extended coverage, especially when evaluating large regions where ground measured data is limited. Other advantages include reliability as it has been accredited free access, to retrieve data without subscriptions.

Also the average monthly maximum and minimum temperatures were measured at 2m height from the ground, which is appropriate for solar PV array on that height from ground. Inter annual single point data of 0.25 $latitude$ × 0.25 $longitude$ grid interval from -31.00 to -28.00 latitude and 27.00 to- 30.00 longitude. The study obtained 169 points, covering the entire area of Lesotho.

Long term monthly averages of minimum and maximum temperature were obtained by averaging each month for the period 2004-2018. The grid data developed was implemented in to solar-pump-pipe sizing computer program, for speedy calculations. Also for temperature the bilinear interpolation was applied to interpolate the points that are not gridded in the data base. The process implementing bilinear interpolation in to the computer program, for faster estimates of temperature magnitudes at any point within gridded database range, for long–term monthly averages of minimum and maximum temperatures was repeated in the same manner as the solar radiation grid data base interpolation program encryption.

The data was also used to produce contour maps of global solar radiation and with the aid of the software Surfer [78]. Surfer is a grid-based mapping program that interpolates irregularly spaced XYZ data. The

mapping software with its ordinary kriging interpolator was used for validation; comparison with results of bilinear technique applied in this case study.

3.3 Optimal sizing of PVPWS.

3.3.1 Evaluating the design month.

Electric energy output of solar photovoltaic (PV) module is affected by its tilt angle with horizontal plane. This parameter changes the amount of solar energy received by the surface of the PV module. Flat-plate collectors are tilted so that they capture maximum radiation [87]. Since the flat-plate solar collectors are positioned at an angle to the horizontal, it is necessary to calculate the optimum tilt angle which maximizes the amount of collected energy all year.

It is generally known that in the southern hemisphere, the optimum collector orientation is north facing and that the optimum tilt angle depends on the latitude and the day of the year. There are many papers in the literature which make different recommendations for the optimum tilt, based only on the latitude [88]. In this study, a collector plate is oriented north facing and at a fixed tilt which is set to maximize the average energy collected over the year [89].To determine daily average solar radiation, Klein's [29] average day of the month as shown in table 4 is applied. Thus long-term monthly average meteorological data is treated as if it occurred on this average day. To determine the fixed optimum tilt angle, radiation on a tilt plane is calculated using several tilt angles that are ± 5 degrees from site latitude.

The tilt factor, which is the fraction of global radiation on the tilted plane to that on the horizontal surface, The tilt factors are listed on Table6 for an optimal fixed collector tilt of $\pm 5^{\circ}$about latitude of 30.36 degrees, Since when increasing the magnitude of tilt angle results in reduced annual energy yield. There are models of tilt angles whereas some researchers suggest two values for the tilt angle, one for summer and the other for winter, such as $\varphi \pm 20°$ [7], $\varphi \pm 8°$ [8], $\varphi \pm 5°$ [90], where φ is the latitude.

The magnitudes of radiation on tilted plane for respective months are listed on table 7. The least producing month is the design month for this present study. The determined design month is June with the least radiation on optimum tilt angle of $+5^{\circ}$ about latitude month yields highest amount of energy collected by PV module.

Table 6 Tilt factors determined for Tosing ±5°about latitude.

Tilt angle	January	Februar	March	April	May	June	July	August	Septembe	October	November	Decembe
25.36	0.94	0.997	1.076	1.215	1.358	1.43	1.417	1.285	1.14	1.022	0.948	0.92
26.36	0.936	0.994	1.076	1.22	1.368	1.433	1.43	1.293	1.142	1.02	0.944	0.914
27.36	0.931	0.992	1.076	1.225	1.378	1.456	1.441	1.3	1.144	1.018	0.939	0.909
28.36	0.921	0.989	1.076	1.23	1.388	1.492	1.453	1.306	1.146	1.015	0.934	0.903
29.36	0.921	0.985	1.075	1.234	1.397	1.492	1.464	1.319	1.147	1.012	0.929	0.897
30.36	0.916	0.982	1.075	1.238	1.406	1.503	1.475	1.325	1.148	1.01	0.924	0.891
31.36	0.911	0.979	1.074	1.241	1.414	1.513	1.485	1.33	1.149	1.006	0.919	0.88
32.36	0.905	0.975	1.073	1.245	1.422	1.542	1.495	1.335	1.149	1.003	0.913	0.879
33.36	0.9	0.971	1.072	1.248	1.43	1.528	1.505	1.34	1.148	0.999	0.907	0.872
34.36	0.894	0.967	1.07	1.251	1.438	1.534	1.514	1.344	1.149	0.996	0.901	0.865
35.36	0.888	0.963	1.069	1.253	1.445	1.544	1.523	1.346	1.149	0.989	0.891	8.858

Table 7 Radiation on tilted plane for Tosing ±5°about latitude

Tilt angle	January	February	March	April	May	June	July	August	Septermber	October	November	December
25.36	6.49	6.19	5.8	5.74	5.27	4.46	5.23	6.01	6.69	6.75	6.94	6.91
26.36	6.46	6.17	5.8	5.76	5.31	4.68	5.28	6.04	6.7	6.74	6.91	6.87
27.36	6.43	6.15	5.8	5.78	5.35	4.76	5.32	6.08	6.71	6.72	6.88	6.83
28.36	6.39	6.13	5.8	5.81	5.39	4.86	5.36	6.11	6.72	6.72	6.84	6.78
29.36	6.36	6.11	5.8	5.82	5.42	4.88	5.41	6.14	6.73	6.69	6.8	6.74
30.36	6.23	6.09	5.8	5.84	5.46	4.88	5.44	6.17	6.74	6.67	6.77	6.69
31.36	6.29	6.07	5.8	5.86	5.49	4.91	5.48	6.2	6.74	6.65	6.73	6.65
32.36	6.25	6.05	5.79	5.88	5.52	4.95	5.52	6.22	6.74	6.62	6.69	6.6
33.36	6.21	6.02	5.78	5.89	5.55	4.99	5.56	6.25	6.74	6.6	6.64	6.55
34.36	6.17	6	5.77	5.91	5.58	5.01	5.59	6.27	6.74	6.58	6.6	6.5
35.36	6.13	5.98	5.76	5.92	5.61	5.05	5.62	6.29	6.74	6.4	6.53	6.45

Figure 9 is the graphical presentation of ±5° tilt of the latitude of Tosing -30.36 latitude ad 29.70 longitude. Also the design month chart clearly shows the optimum tilt angle 35.36 yielding maximal energy of all sampled tilt angles.

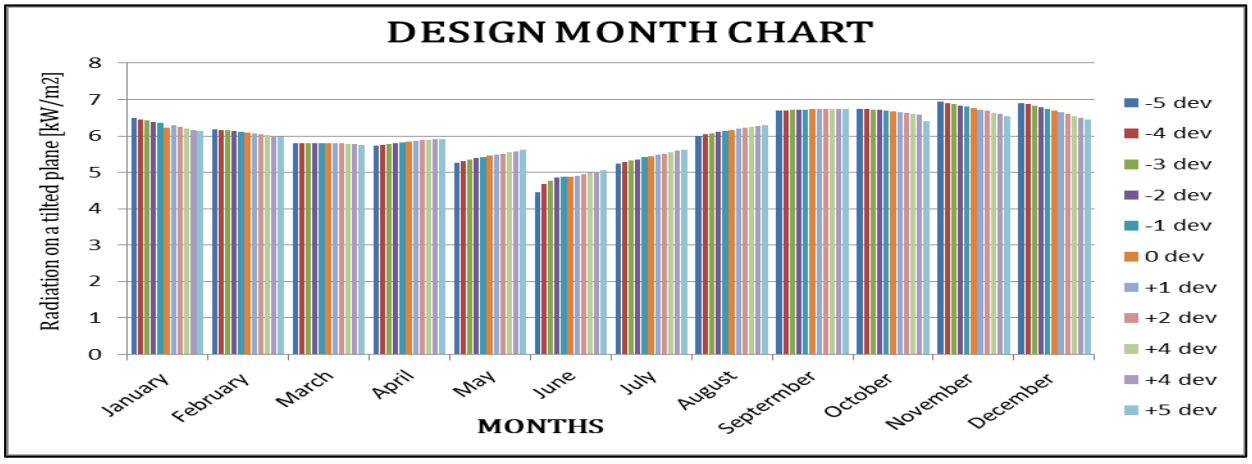

Figure 9 The design month chart.

3.3.2 System components sizing and deriving Flow-Power Functions.

In conventional water pumping applications where the pump operates at constant frequency all the time, it is simple to find suitable pumps by comparing their instantaneous efficiencies at grid frequency (50 Hz or 60 Hz) given in the manufacturer pump data sheets. For given water the optimum pump will be the one that gives maximum efficiency for the corresponding well head. In PV water pumping, the situation is not the same. The diurnal changes of radiation, the nonlinear behavior of efficiencies of subsystems and flow rate with solar output and the sensitivity of system performance to system operating head and PV array size are the main parameters that significantly affect the design, optimization and rating of PV pumping systems. An accurate design and optimization will not be ensured by considering only ordinary manufacturer's data charts or using other methods applied for other applications such as the utilizability concept [75].

Simple methods where, firstly daily water demand, the required pump flow rate is obtained by dividing the daily demand by the effective peak sunshine hours, for the month receiving the least tilted-radiation, do not hold for optimal sizing. A major problem in the design and implementation of PV pumping systems is that each component of the system has its own operational characteristics that are not necessarily beneficial to the next component [40]. Performance of PV pumping systems degrades as insolation decreases from its nominal design point [91]. A proper matching of a pump and pipelines at a set hydraulic load to the PV array output is a great problem [92].

It is an objective of this study to derive pump power-flow functions that relate PV power to flow-rate ("wire to water) relation. The models reviewed [53, 56]; do not give a direct relationship between the operating electrical power of the pumping subsystem and the water flow rate of the pump. However, these models are based on the characteristics of each component that are available from the manufacturer data, the available analysis methods are based on sizing system components separately, which can cause mismatch of components. In addition reviewed methods consider only the efficiency at the maximum operating frequency but not the whole range of operating frequencies.

3.3.2(a) solar pump selection and deriving iso-power Head-Flow (H-Q) pump curves.

(i)Solar pump selection

The selection of a pump mainly depends on the head of operation, total water output required per day, flow rate and pump-system efficiency at head of operation. To find a suitable pump for given operating conditions as shown by table 8, the process should start with the preliminary selection of the pump by determining design flow-rate, which is calculated by dividing daily water requirement with location peak sunshine hours.

From site information, the daily water demand is 350m³/day dividing by design month peak sun shine hours, which are 5.051 as determined from table 3.07 of radiation on tilted plane for Tosing at +5°about latitude. The design flowrate is 69.3m³/hr the next step is to determine operating head for this application.

The design of 60m static head, frictional losses must be added to find the total dynamic head. The friction loss h_f is calculated for design flow rate by online calculator at https://goodcalculators [93].Friction loss calculator employs The Hazen-Willam formula [72]; Frictional losses in are calculated on the basis of known flow rates in circular pipes, known internal diameter of a pipe and length of a pumping mains. The Hazen–Willam coefficient in is set at C=135 *(see annex 3),* for this study. Coefficient will vary over a pipe's life time as such informed judgments are made when choosing the appropriate coefficient. The diameter of the pipe required for this current application is determined firstly by assuming a velocity of water is 1m/s and flow-rate is 0.0193m³/. Since $Q = AV$ where $A = \pi D^2/4$ and $D = \sqrt{0.0193} \times \frac{4}{\pi}$ =0.157m≈ 0.160 m, therefore the required standard pipe is 160mm diameter pipe. Calculating the frictional losses for specified parameters yields 18.00 m and therefore TDH is 78m.

With this information of known TDH and corresponding design flow-rate, the desired manufacturer is selected. Lorentz pump products [70];are reliable and the complete, efficient, solar water pumping solution using performance chart from selection table 8; of website; www.Lorentz.de./partners.com.

Table 8 Lorentz pump products selection table

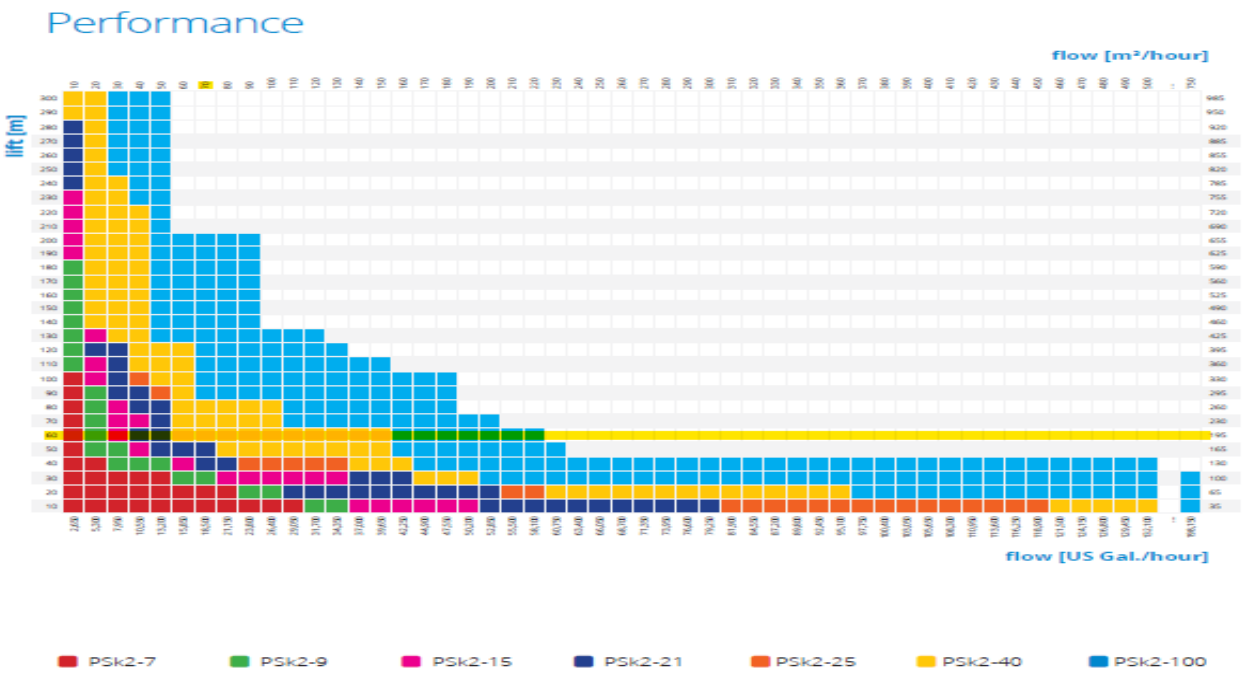

(ii) Deriving Iso-Power Head-Flow (H-Q) Pump Curves

Reputable solar pump manufacturers normally provide laboratory tested data of the pump performance characteristics such as shown on Figure 10 illustrating iso-power readings.

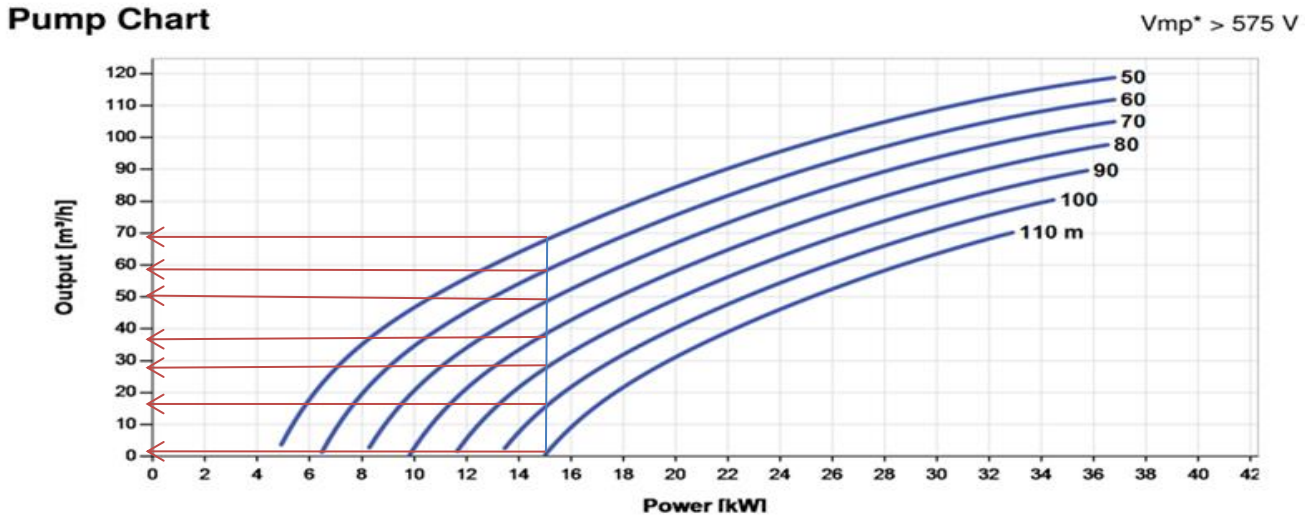

Figure 10 Readings of corresponding H-Q iso_power.

It is impractical for a manufacturer to supply system output data for infinite combination of the solar output and the pumping head. The provided pump characteristic curves show the variation of the pump flow rate (*Q*) reacting to the variation of power supplied by the PV array (*Ppv*) for a given (constant) total dynamic head (*TDH*).

In this format, the pump data is not sufficient enough to enable the prediction of pump performance, Moreover, the system output varies with the various combinations of the system components (photovoltaic module, pump, various pipes and their fittings and water storage size) that a system may be comprised. It is therefore necessary to develop a model for a pumping system that can predict the output for any combination of head and PV power and flow rate. Firstly the relation of head and flow rate as shown by equation 5:

$$H = p_2 Q^2 + p_1 Q + p_0 \qquad \{enq.5\}$$

is analysed using the provided pump performance. The objective is to determine the regression coefficients of pump at given PV power. For each selected PV power supply level as illustrated by Figure 10, a pump *H-Q* curve are defined by observations and recordings of dual matching of *H* and *Q* values from figure 9. To determine the specific regression coefficient of the pump (*p0, p1, p2*), the curve fitting technique is applied to determine best fitting curve. The best trend line is the second degree polynomial, the pump-specific regression coefficients *p*, *p1* and *p2* are given in table 9; for respective PV power of figure 10 and where *Q*

[m3/hr] is the flow rate. The *H-Q* curves are plotted on Figure 10, showing corresponding correlation coefficient R^2

Table 9 H-Q specific regression coefficients for Lorentz PSk-2-40-C-SJ95-7 solar pump

PV power	**15kW**	**16kW**	**18kW**	**20kW**	**22kW**	**24kW**	**28kW**	**30kW**	**32kW**	**32kW**
p0	97.71	102.14	120	130	130	131.86	139.57	145.71	148	148
p1	-0.3595	-0.4262	-0.7088	-0.9	-0.7655	-0.7155	-0.656	-0.7429	-0.6976	-0.6976
p2	-0.0048	-0.0038	-0.008	-1	-0.0006	-0.0006	-0.0008	-3	-0.0002	-0.0002

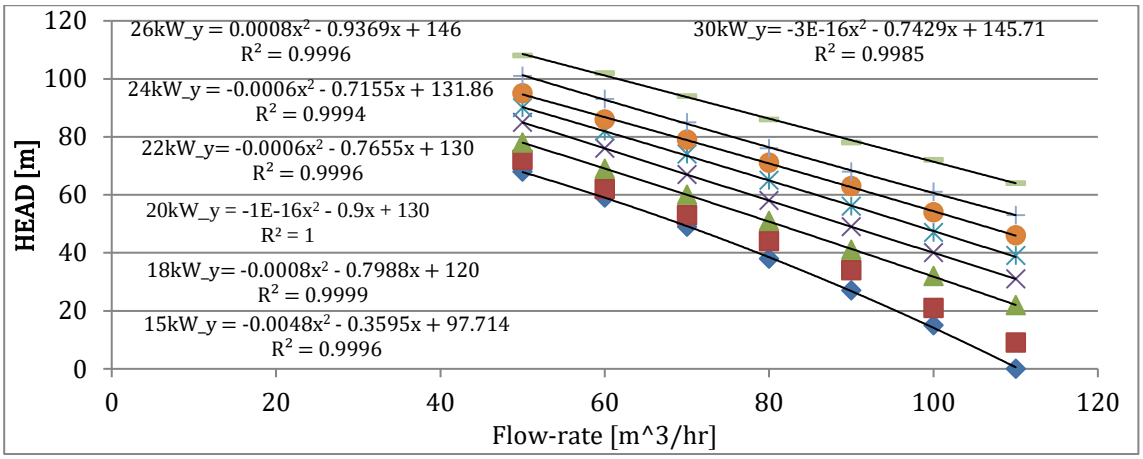

Figure 10 Pump H-Q curves for different PV power.

The H-Q curves clearly demonstrate the model agreement with affinity laws of the first premises which relates the speed of the pump to the required PV power. H-Q curve will be different for different power (different pump speeds) according to pump affinity laws.

3.3.2(b) Pipe system selection and sizing and evaluation of system resistance.

(i) Pipe selection

Modified Poly Vinyl Chloride (PVC-M) Pressure Pipe Systems is a tough and resilient, modified PVC pressure pipe, developed for greater strength, as such PVC-M is the study design piping material [94]. The sampled pipe were based on estimates of water to deliver, also of all pipes sampled class 10 is selected (*see: annex 2)*, after class 6 which is limited to operating head less than 60 meters, thus class 10 pipe can operate at the designed head of the present study.

The amount of water pumped for each sampled PV-pump-pipe design is obtained by computing the monthly-average daily volume pumped multiply it by the number of days in each month and then summing the

monthly delivered volumes over the year and dividing by total cost of the system's life. The PV-pump-pipe design resulting in the lowest cost of pumping calculated as above is the objective optimal choice for the solar pump system design. The choice of the PV-pump-pipe design is dependent on pipe sizes, since a larger diameter pipe (large pipe costs) requires a smaller PV array size (small PV array costs). In practical, the size of the pump may also vary for different pipe diameters used to perform a given pumping duty, therefore varying the cost structure of the PV-pump-pipe system.

(ii) Analysis of system resistance curve.

The parameters of equation 6, system *resistance (TDH)* represents the total dynamic head of the pump, H_0 is the static head and h_L (friction and minor abrupt losses).

$$TDH = H_0 + H_L \qquad \{enq.6\}$$

For long pumping mains, the minor losses tend to be very small and may be neglected, and the friction loss h_f is conveniently calculated for each flow rate by online calculator at https://goodcalculators [93]. Friction loss calculator employs The Hazen-Williams formula [72]; given in equation 7is used.

$$V=0.85C\left(\frac{D}{4}\right)^{0.63} S^{0.54} \qquad \{eqn.7\}$$

Frictional losses in pipes are calculated on the basis that; flowrates are in circular pipes, of known internal diameter of a pipe and length of pumping mains. The Hazen–Willam coefficient in equation is set at C=135, for this study. Coefficient will vary over a pipe's life time as such informed judgments are made when choosing the appropriate coefficient. However in the list of materials and their Hazen-William coefficient is C=150 (*see annex 3*).

The "system curve" is a graphical illustration of the relationship between the pumping head, taking into consideration the pressure losses in the pipes of the pumping system, and the flow rate. It is completely independent of the pump characteristics and its basic shape is parabolic, If H_{00} is zero, it will start at the point zero water flow *(Q)* and zero pumping head *(H)*; otherwise the curve will be vertically offset from the zero to appropriate H_0 [91]. The system resistance curve *TDH* is plotted on Figure 11; for a static head of 60 m and pumping distance 3000 m, and for 125mm, 140 mm,160mmm, 177mm 200mm Southern Africa standard diameter PVC pipes, respectively [94].

The total dynamic head can be conveniently expressed by quadratic equation shown in equation 8.

$$TDH=H_0+h_1Q+h_2Q^2 \qquad \{eqn.8\}$$

To determine the system coefficients *h1* and *h2*, the curve fitting strategy is applied to determine best fitting curve. The best fitting line is of the second order polynomial expression, the system coefficients are presented in Table 10 for the respective pipe sizes and the appropriate correlation coefficient R^2 values are shown in figure 11 of the system curve.

Table 11 System resistance head coefficients

Pipe diameter	200mm	177mm	160mm	140mm	125mm
h1 [hr.m^{-2}]	0.134	0.006	0.041	0.025	0.008
h2 [hr.m^{-5}]	0.0106	0.0796	0.0032	0.0019	0.0011

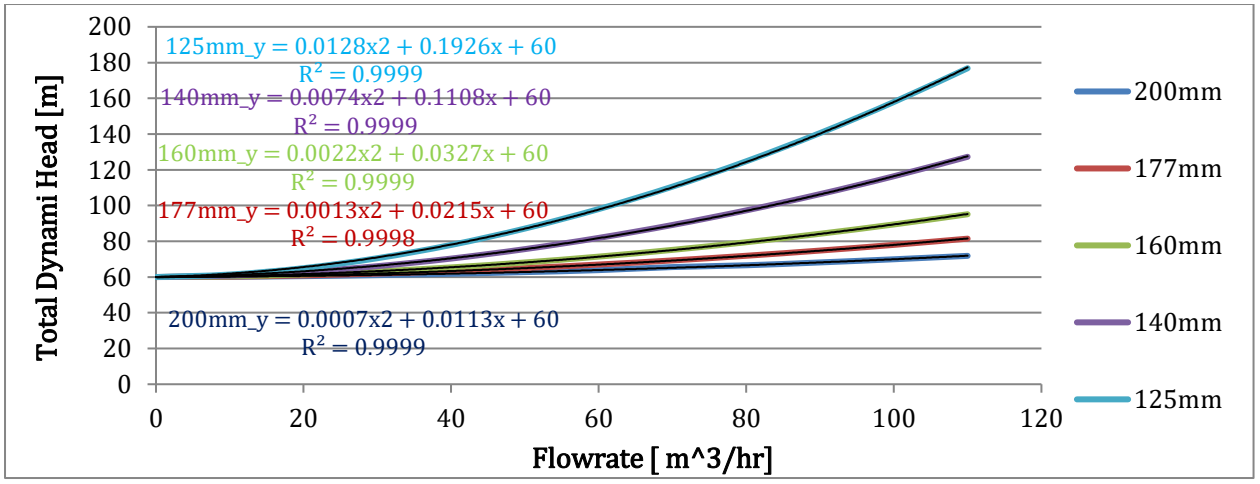

Figure 11 System resistance curves for different pipe diameters.

3.3.2 (c) Sizing solar PV array

(i) Deriving the operation flow-head-power functions of the PV pump.

TDH for a pump is the sum of the vertical lift, pressure head, and friction loss. Friction losses apply only to the piping and appurtenances between the point of intake (inlet) and the point of storage (i.e. the storage tank or pressure tank). Flow from the storage tank to the point of use (i.e. the trough) is typically gravity fed. Therefore, friction losses between the storage tank and the point of use are independent from the pump and do not need to be accounted for when sizing the pump.

However there is a need to find points where the system intersects with pump performance curve to find the actual pump-system operating points. They may be obtained analytically as the simultaneous solution of equation 5 and 8.

$$H = p_2Q^2 + p_1Q + p_0 \qquad \{enq.5\}$$

$$TDH = H_0 + h_1Q + h_2Q^2 \qquad \{enq.8\}$$

The operational points are given by the following quadratic expression, which can be cumbersome for practical designs. This equation shows the non- linear operation of system's components.

$$Q_{op} = MAX[0, \frac{(h1-p1)\sqrt{(b1-h1)^2-4(p2-h2)(p0-H0)}}{2(p2-h2)}] \qquad \{eqn.9\}$$

$$TDH_{op} = H_0 + h_1 Q_{op} + h_2 Q_{op} \qquad \{eqn.10\}$$

From equation 9 and equation 10, TDH_{op} is the total dynamic head at operating point and Q_{op} is the operating flow rate. Alternative method is the use of pump curve in figure 10 and the system curve in figure 11 superimpose the system characteristics curve on the pump characteristics curve as shown in Figure 12. The operating points are the intersections of the system curve and the pump when connected to 125mm, 140mm, 160mm, 177mm and 200mm pipe line diameters for 3000m length

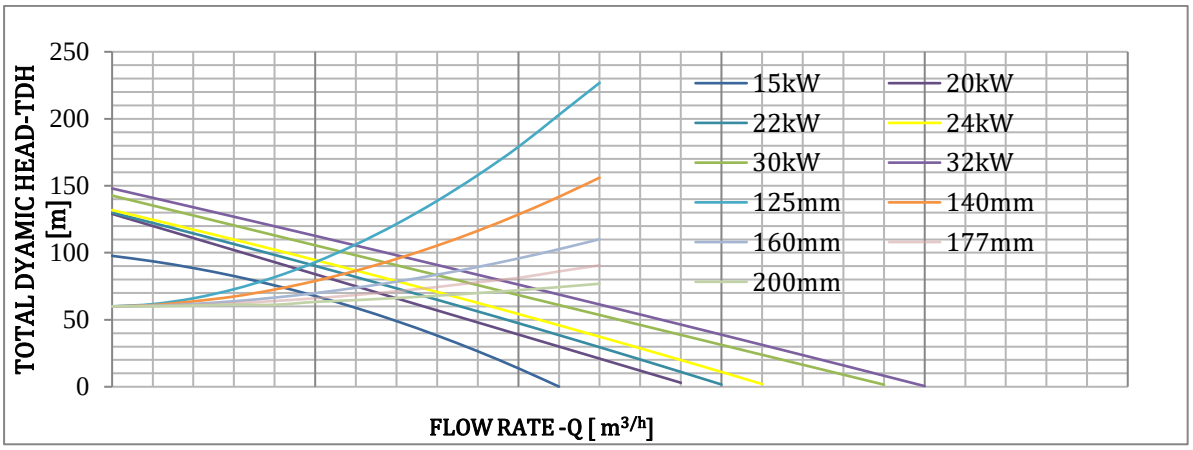

Figure 12 Pump H-Q curves (downward sloping) and system curves (upward sloping) for 5 different pipe diameters

The results derived from figure 12 of superimpositioning of the system characteristics curve on the pump characteristics curve, are the operating points of the system curve and the pump when connected to 125mm,140mm,160mm, 177mm and 200mm pipe line diameters for 3000m length.

(ii) The sizing of PV array

Using computer program; the sizing of PV array is achieved by iteratively varying the range of power values until the desired daily flow volume is obtained, for the design month. PV power required for specified radiation on PV module G_{pv} is obtained by the application of equation 13:

$$P_{pv} = \frac{\eta PV}{\eta STC} * \frac{Gpv}{G\ sTc} * P_{STC} \qquad \{eqn.13\}$$

To determine the hourly PV power required, the hourly values are determined by calculations of long term monthly averages of global horizontal radiation. They are distributed to daily averages by Klein's average day dates [29].

From daily averages the hourly radiations tilted plane are computed ,by application of justified and simplified sky model [27]:The flow rate per hour is directly determined from the flow-power functions described by equation 11:

$$Q_{op} = q1\ln(P_{pv}) - qo \qquad for\ P_{pv} \geq P_{off}$$

$$Q_{op} = 0 \qquad for\ P_{pv} < _{off} \qquad \{eqn.11\}$$

The PV array power output is varied in small intervals until the required daily pumped volume of water of 350 m3/day is obtained. The simulation process is doe firstly for the design month of June, which is the lowest in production in terms of average daily water yield on annual basis for Tosing, Lesotho. The PV power output values required to deliver 350m³per day are recorded and presented in table 11 section. The processis repeated for all pipes sampled.

Table 11 PV power required to deliver350m³/day of water for different pipes.

Pipe diameter	125mm	140mm	160mm	177mm	200mm
PV power required	25360W	22260W	20010W	18906W	17355W

(ii) PV power configuration

The selection depends on its nominal operating power and voltage. The required PV array is optimized further by matching the maximum pump rated voltage $V_{rmp} > 575$ for the selected pump. Table 13 shows the electrical parameters of seleceted TTN-295-315M72 monocrystalline solar module [96]; for this study

Table 12 Electrical data of TTN-295-315M72 monocrystalline solar module

Electrical data					
Nominal Power Watt Pmax(Wp)	295Wp	300Wp	305Wp	310Wp	315Wp
Power Output Tolerance Pmax(W)	0/+5	0/+5	0/+5	0/+5	0/+5
Maximum Power Voltage Vmp(V)	36.34V	36.59V	37.02V	37.31V	37.64V
Maximum Power Current Imp(A)	8.12A	8.2A	8.24A	8.31A	8.37A
Open Circuit Voltage Voc(V)	45.5V	45.6V	45.7V	45.81V	45.91V
Short Circuit Current Ioc(A)	8.7A	8.78A	8.82A	8.87A	8.94A
Module Efficiency m(%)	15.25%	15.50%	15.76%	16.02%	16.28%
Maximum system voltage	1000V				
Operating temperature	-40℃ to+85℃				
NOCT	45℃ to ± 2℃				
Temperature coefficient of Isc	+0.05%/ ℃				
Temperature coefficient of Voc	-0.34%/ ℃				
Temperature coefficient of Pm	-0.42%/ ℃				
Specifications included in this datasheet are subject to change without prior notice					

For this study the configugaration of 16 parallell modules and 5 mudules in series was attained, by optimal configuration to avoid unnecessary costs. The PV power of 22260 W requreired for 140mm diameter pipe is read from table 12. The electrical data from PV manufacturer shows 36.59 rated voltage of sampled PV module at 300W. Set 600 volts rating to match pump rated voltage. $600 \div 36.59 = 16.39 \approx 16$ modules are requrired at least.the number of strings required $22260 \div 300 = 4.49 \approx 5$ series strings, thus total of 80 modules. Then $80 \times 300 = 24000$W PV array is required. The magnitude of deviation from design point is 24000Watts devided by 22260Watts, that is 1.1% deviation from design point, thus ovesizing is avoided in this study.

3.3.4 Cost of pumping.

It is essential that economic analysis should be made while optimizing the size of solar water pumping favoring an affordable unit price of water produced. The economical approach, according to the concept of life cycle cost (LCC). The LCC is defined as the total cost of the whole PVWPS. Life cycle cost (LCC) analysis, illustrated by Brandumahel [95], is opted the widely used method for evaluating the cost of a desired system. Life cycle cost analysis gives the total cost of the PV powered water pumping system including all expenses incurred over the life of the system, and it is helpful for comparing the costs of different system designs.

A PVWPS can operate for a period of time before it needs replacement, the PV panels may be replaced after 20–30 years, yet the pump may be replaced after 5–10 years. The life cycle costs of a PV pumping system are the capital expenses of the whole system from the date of installation plus the annual operation, and maintenance expenses.

The life cycle cost analysis consists of finding the present worth of any expenses expected to occur over the life cycle of the system. The effects of different system components with different reliabilities and lifetimes can be evaluated using LCC analysis. In LCC analysis, the present worth value of all the capital and recurring costs for the PV powered pumping system is calculated. The present worth of a future, in a given year (n) at a given discount rate (r %) is given by equation 16's middle parameter. Four main parts are considered: PV array, the solar pump system and pipe system and operations and maintenance costs. In order to make an objective selection of the pipe size to use in the solar-powered pump-pipe system, it is necessary to determine an objective-function metric to use for comparison.

The comparison metric used in this paper is the *unit cost of pumping*. The unit cost of pumping is calculated as the annualized cost of the sum of capital costs of the solar PV array; the pipe line and the pump-motor-controller unit, plus the annual maintenance costs, all divided by yielded volume of water pumped. For each capital asset of the pumping system, the annualized cost is calculated from equation 16. At a set discount rate of $r=$ 10% discount rate, this means that a \$100 cost today may be considered equivalent to a \$110 cost incurred 1 year from today and an asset lifespan of n years depending on components, as outlined by.

$$C_{\text{COST OF PUMPING}} = C_{\text{CAPEX}} \times \frac{r}{1-(1+r)\text{^}-n} + C_{\text{OM}} \qquad \{\text{eqn.16}\}$$

From manufactures and suppliers the pricelists, technical specification of PVWPS components, are requested for analysis to evaluate variables of equation 16. The PV panel prices are available online at: https:www.enfsolar.com [96]. The Lorentz PSk-2-40-C-SJ95-7 solar submersible water pump system prices were retrieved from https://www.alibaba.com [97]. The pipe lines and their fittings were retrieved from http://www.kuzeyboru.com [98].

Cost information of the major components are as following, the cost of PV modules fluctuates greatly on the market but has declined gradually in recent years. For the world market, the up-to date PV module price is 0.24/W [96]. In this study, the initial capital cost of a PV module is assumed as \$0.46/W, including the installation costs. The system life is assumed as 25 years. A summary of the cost information about the main components and their corresponding lifespan is presented in Table 13. The Lorentz PSk-2-40-C-SJ95-7 solar submersible water pump system price is \$465.00/kW [97] and the design pipe is 140mm diameter and 3000m length M-PVC pipeline \$9.18 [98].

Table 13 Cost components information *(for more details see Annex 1&2)*

Item	Unit	Cost	Lifespan(years)
PV module	W/m	$0.46/W	25
Pump	34kW	$465/Kw	10
Pipelines	Meters[m]	$9.18/m	40

The expenses of transportation, construction and operations and maintenance are also considered for evaluation. The prices of solar water pumping system components are adjusted such that all cost encountered, from factory price to implementation stage are analysed: The prices are calculated using equation 15.

3.3.5 Storage design.

The fundamental goal of a solar-powered water pump system is to store water, not electricity. The use of batteries should therefore be avoided unless absolutely necessary since the added expense and complexity usually outweighs any advantages. Water storage is suitable for this application of solar water pumps. Water supply systems are designed to contain (2 to 5 outages) dark days multiplied the average daily water demand.

For variable PV power output the traditional method does not hold as it could lead to over sizing of the storage tank. The mass balance curve approach is applied in this study for the design of 350m3/day storage for sustainable water suppl. The researchers Khatib [68] and Hove [17] demonstrated the mass balance curve method. The model is applied for hypothetical study of Tosing potable water supply scheme. From long term meteorological data, the method estimates the water balance of from daily water demand and the annual production of water for the design month of June. The model stipulates that, since there are some days of poor water yield, with those days with largest water requirement is exactly the minimum size required for storage.

To design the storage, Blokker [99], water stochastic drinking water demand model with small temporal and spatial scale for community supply is used for analysis. First the graph hourly variations of the required water supply and the demand hourly are plotted as shown figure 13 using Blokker. The cumulative graph of both demand and supply graph are also plotted as shown on figure 14. The quantity of water required to be stored in the reservoir for balancing variable demand against (balancing storage) can be worked out by mass curve method [17]. It is calculated from figure 14; as the cumulative of maximum deficit plus maximum

surplus. From figure 14; the balance is evaluated by subtracting withdrawal from surplus ad maximum surplus is the largest gap between the graphs;

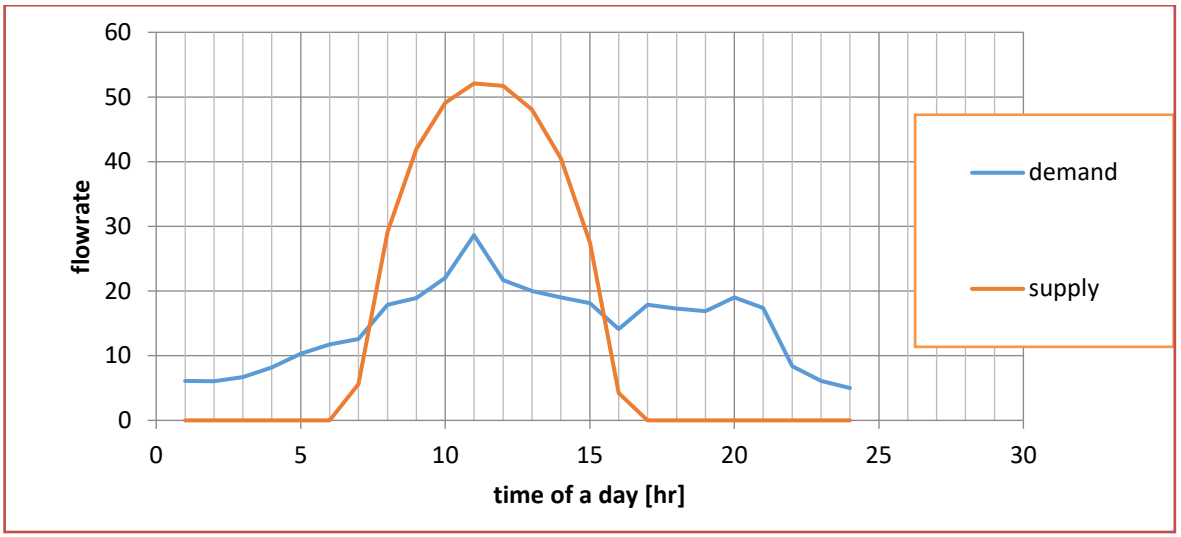

Figure 13 Hourly flowrates of the Solar PV water pumping system

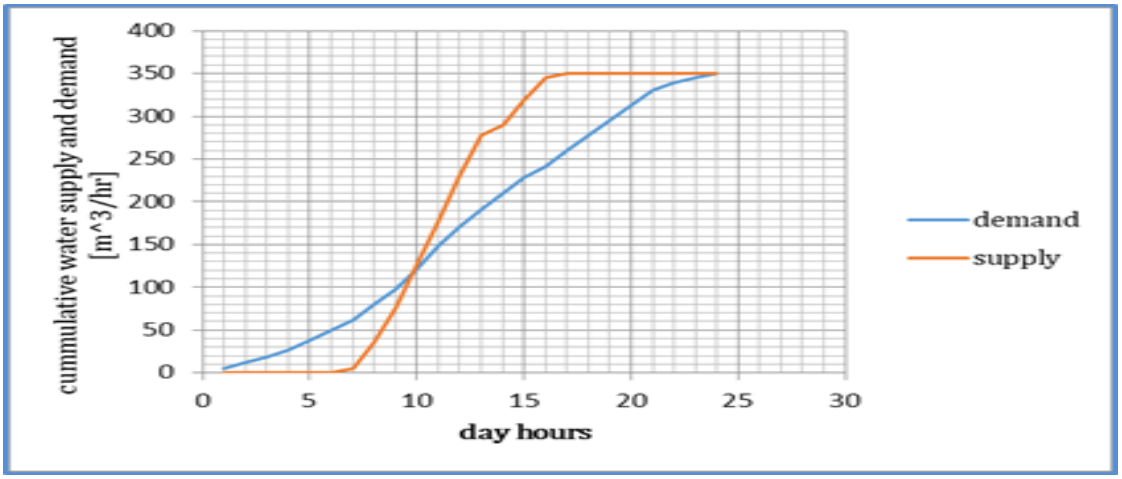

Figure 14 Deficit –Surplus Balance curve for the Solar PV water pumping system.

Thus from the graph: maximum deficit: 60[m^3 hr] -5 [m^3 /hr] =55[m^3 /hr]

Maximum surplus: 345[m^3/hr] – 240[m^3/hr] =200[m^3/hr]

Balance of storage = 255[m^3/hr] is the 57% of daily water demand.

CHAPTER 4: RESULTS AND DISCUSSIONS

4.1 Design-system parameters performance analysis

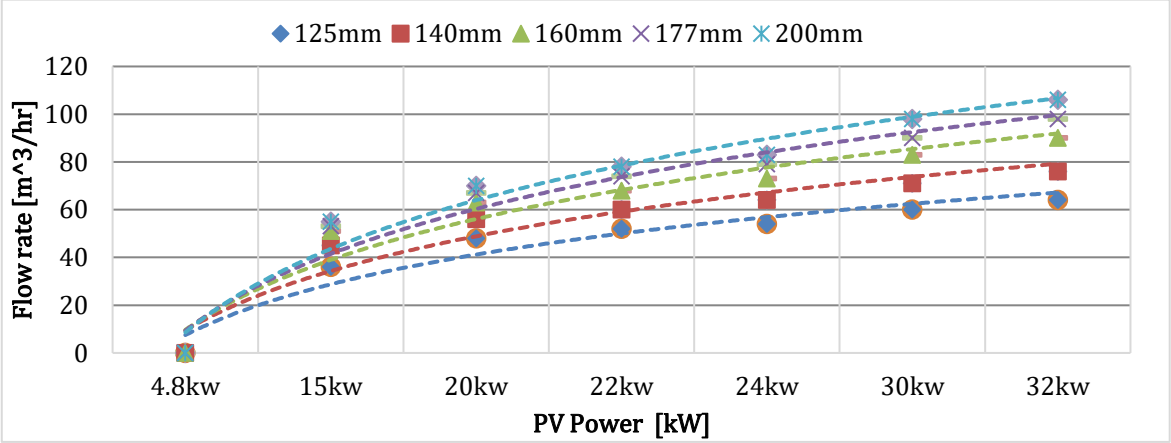

Figure 15 Flow rate to PV-power response functions for different pipe diameters.

Table 14 Coefficients of the flow-power function eqution 11 for the Lorentz PSk-2-40-C-SJ95-7 solar pump coupled with to 3000 M-PVC pipe length of different diameters and for 60 m static head.

Pipe diameter	125mm	140mm	160mm	177mm	200mm
q	28.31	33.38	38.37	43.16	47.24
q_0	-26.21	-35.56	-44.12	-51.63	-63.60

The plotted intersection points from figure 12 are presented in following section of this study. From the litrature review chapter the flow-power relation of the duty points of the solar pump system is expressed by equation 11: The coefficients $q0$ and $q1$ of equation 11 are given on Table 14 and are plotted on Figure 15 for the proposed Tosing water supply pumping system, a system pumping through 3000 m long 125mm, 140 mm, 160mm,177mm, 200mm diameter M- PVC pipes on a vertical height of 60m. From figure 15 The flowrate response in a natural logarithimc manner to PV power output and it depends on system resistivity of different pipe diameters. The operating points are wide range of operating frequencies. Also the cut off power is at 4.8 as also identifying the lowest operating head the system as shown by figure 16, of the threshold PV power required to start the Lorentz PSk-2-40-C-SJ95-7 solar pump, for designer and the user this is important.

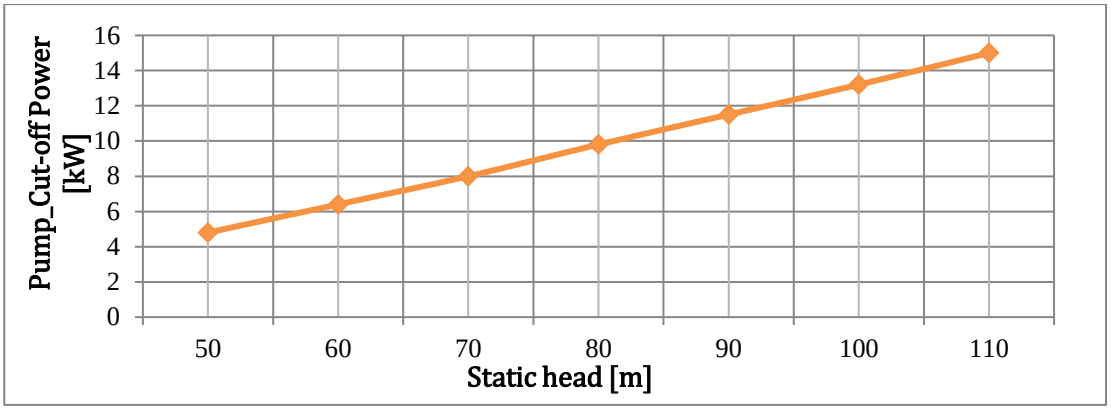

Figure 16 Minimum PV power required to start the pump the (PS21k2 CS-F42-40 solar pump as a function of the static head.

There is a need identify the lowest operating frequency at which the pump is able to elevate water into the storage. It will be defined by the H-Q curve with the lowest frequency that intersects with the system curve. The pumps operating with the lowest frequencies will be preferable, as they will allow a wider range of operating frequencies [91].Unlike conventional methods which maximise the single duty point, the method applied shows the direct relation of variable PV output to flow-rate response,depending on parameters of the pumping mains.It PV power being the driver, it is subjcted to response to variable, priodical and predictable climatic factors [23].

Table 15 Design data for 140mm solar PV_ pump-pipe water system, for Tosing water supply, Lesotho.

LOCATION	PIPE-SYSTEM	PV power system	PUMP SYSTEM
Latitude:-30.36 Longitude:27.90	Static head:60m	Type: monocrystalline silicon solar.	Max head:110m
Design month: June	Pipe diameter: 140mm	V_{PM}: 37.12V	Max flowrate:119[m^3/hr]
Global solar radiation: 3.29kW/hr/day	Pumping main length: 3000m	η_{STC}:16%	Vrmp: >575
Maximum temp:12.5°C Minimum temp:-1.03°C	h_1: 0.025	β: 0.004/°C	q: 33.38
Village:Tosing,Quthing	h_2: 0.002	T_{NOCT}: 46°C	q_o : -35.56
Water source: Borehole well	Pipe-material: PVC	Required power:22260W	Submersible solar pump

The design data for performing computations of Solar Pump Performance and determination of required PV array size for the present case study are presented in table, where the pump is connected to 140mm diameter pipe. The simulations of hourly variations of 140mm pump mains system parameters are shown on table 16.

Table 16 Performance parameters of 140mm pipe

TIME		G	Ta	Tc	ηPV/ηREF	Ppv	Qop [m3/h]	THD	ρgQopTDHo	Ηpump	Ηover	Ηpv
05:00-06:00												
06:00-07:00	6.5	0	-0.4	-0.4	0.99	0	0.000	60.0	0	0.0%	0.0%	0.00%
07:00-08:00	7.5	152	-1.0	3.2	0.98	3316	4.456	60.2	730	22.0%	3.3%	15.20%
08:00-09:00	8.5	324	-0.3	8.6	0.96	6927	29.043	62.4	4940	71.3%	10.6%	14.89%
09:00-10:00	9.5	494	1.6	15.2	0.94	10293	42.265	64.6	7444	72.3%	10.5%	14.51%
10:00-11:00	10.5	630	4.3	21.6	0.91	12797	49.532	66.1	8928	69.8%	9.9%	14.15%
11:00-1200	11.5	706	7.3	26.6	0.89	14041	52.629	66.9	9588	68.3%	9.5%	13.86%
12:00-13:00	12.5	706	9.9	29.3	0.88	13886	52.259	66.8	9508	68.5%	9.4%	13.70%
13:00-14:00	13.5	630	11.8	29.1	0.88	12410	48.507	65.9	8713	70.2%	9.6%	13.72%
14:00-15:00	14.5	494	12.4	26.0	0.90	9854	40.810	64.4	7156	72.6%	10.1%	13.89%
15:00-16:00	15.5	324	11.8	20.7	0.92	6606	27.462	62.2	4654	70.5%	10.0%	14.20%
16:00-17:00	16.5	152	9.9	14.1	0.94	3180	3.058	60.1	501	15.7%	2.3%	14.57%
17:00-18:00	17.5	0	7.3	7.3	0.97	0	0.000	60.0	0	0.0%	0.0%	0.00%
TOTAL VOLUME		**4611**	**6.2**	**16.8**	**0.93**	**95487**	**350.0**	**63.29**	**62162**	**0.50**	**7.1%**	

The results of 140mm pumping mains performance shows: The hourly flow-rates when computing integration over hourly intervals, for sunshine hours are evaluated by the applied sky model:

$$G_T = G_b R_b + G_d \qquad \{eq.1\}$$

The integral result in the daily water volume delivered by the pump is function of The PV array power output is adjusted, until the monthly-average daily volume of water delivered is achieved. The required PV array power output was varied in small intervals until the required daily pumped volume of water of 350m3/day is obtained. The performance table 16 demonstrated how the PV array size was determined when the solar pump response when connected to; 140 mm diameter pipe of 3000 m horizontal length and 60 m static head.

The average of solar PV array efficiency $\bar{\eta}_{pv}$ is evaluated as the sum of the hourly PV power over the day divided by the sum of hourly irradiance multiplied by the PV array area. Similarly the average pump efficiency $\bar{\eta}_{pump\_op}$ is the sum of the water power output $\Sigma \rho g Q_{op} H_{op}$ divided by ΣPpv. The overall average solar-to- water efficiency $\bar{\eta}_{overall}$ is then $\bar{\eta}_{pv} \times \bar{\eta}_{pump\_op}$. There are several parameters which affect the performance of PVWPS but, the total dynamic head (TDH), flow rate (Q), solar radiation (G) and PV power are most important. The graphical results of modeled hourly variation of the flow-rate Q[m^3/hr]-total dynamic head TDH [m] relation, for the design month (June) of system with 140 mm diameter pipe and 22260 Watts PV array power are shown on figure 16 on the average day of June.

Observing figure figure18 system starts pumping at around 06:30 a.m. from 60 meters static head, the flow rate increases gradually from 4.46m3/hr, with increase in radiation up to noon hour's peak power, remains constant during the noon hour and rapidly falls during the late part of day after 13.30 p.m. Depending on the solar irradiance and total head, the flow-rates varied between 3.06 m^3 and 52.63 m^3 on that average day as seen table 15. The results prove that as the flow rate increases there is increase in the total head of the pump.

The simulated results, from the applied Hove model, displaying efficient and clear parametric analysis of system's response to hourly time step of the main parameters affecting the system performance are shown in figures that represent. The modeled hourly variation of the solar-pump and overall system efficiencies for 140 mm diameter pipe and 22260 Watts PV array power are shown on figure 17 on the average day of January time step variation of total system efficiency for the design month of (June) at Tosing, Lesotho.

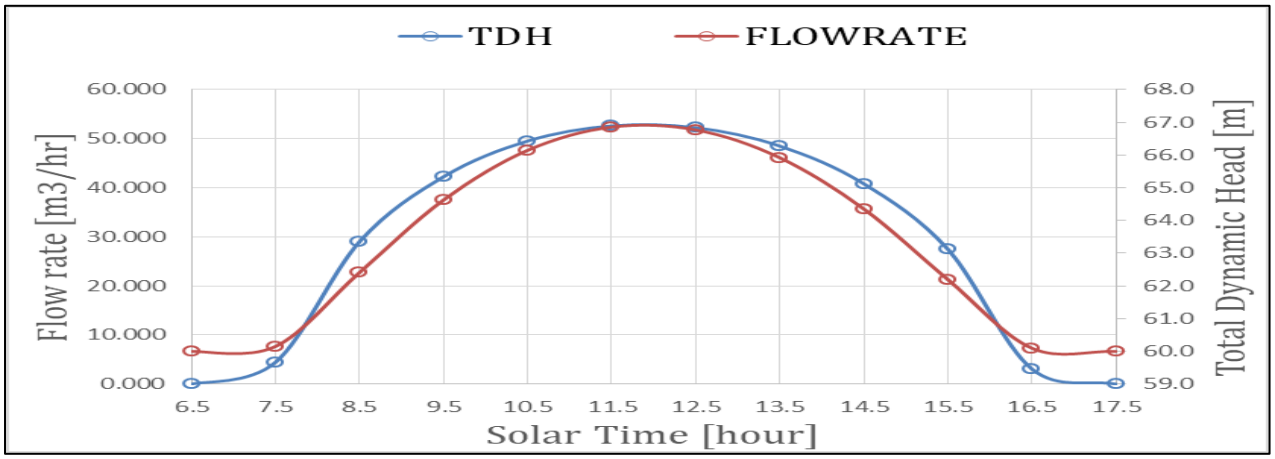

Figure 17 Hourly variations of FLOW-HEAD relation, for the design month (June)

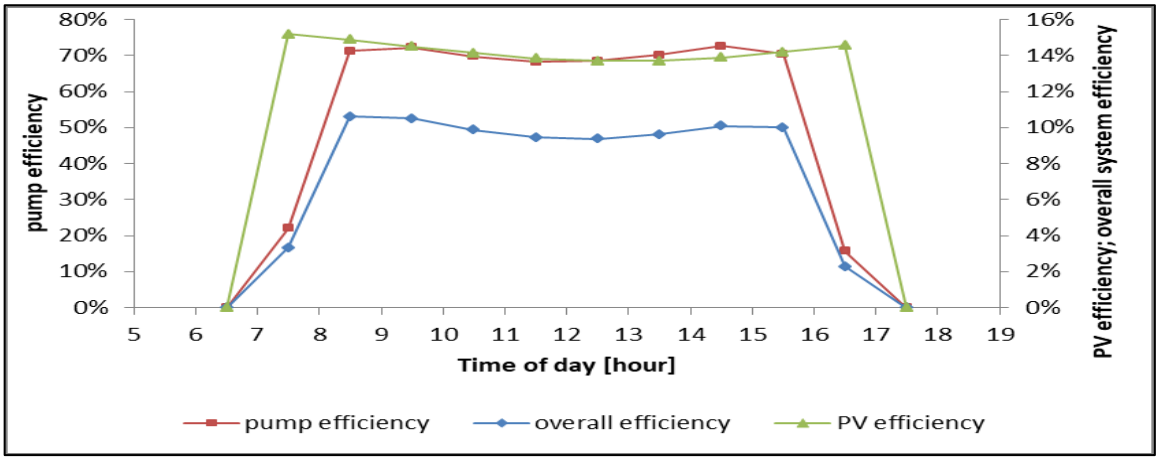

Figure 18 Time step variation of total system efficiency for the design month of (June) at Tosing, Lesotho

The PV efficiency of equation 10: rises sharply from zero 06:30 hours in the early morning and fall to zero at 17:00 hours in late afternoon, due to sun rise and sun set hour.

$$P_{pv} = \frac{\eta PV}{\eta STC} * \frac{Gpv}{G\ sTc} * P_{STC} \qquad \{eqn.13\}$$

The ambient and cell temperatures are low, than in the early-day hours, but when the ambient and cell temperatures are higher.as shown by figure 18 and table 15. the PV. Also Boutelhig et al. [100] concluded that the relationship between PV module temperature and PV module efficiency and is that efficiency decreases with increase in module temperature.

The efficiency of a pump depends on the operating frequency as illustrated by figure 18. The pump efficiency rises sharply during the early hour of 06:30hours to 07:30hours, reaching over 70% efficient. Steadily reduced during midday, rising steadily, to above 70 % but not reaching morning peak, falling steadily at sunset. Observing figure 18 the graph of pump efficiency shows the influnce of the flow-rate and TDH of the system. The overall solar pumping system efficiency increases fairly rapidly from zero in the early morning, peaks in the mid-morning (when the product of PV efficiency and pump efficiency is highest) and then reduces gradually over most of the day, before it falls at sun set.

From figure 19; the designed system's overall efficiency is 7.2% with minimum of 0.0% and maximum performance of 10.1%. The relationship is observed from figure 18; that at 12:30hours the system's curve does not increase with the increase with the same magnitude as pump efficiency, however it seen that the PV efficiency is affecting system overall performance, this is because of increase of critical temperature, in the late afternoon, as equation 13 prescribed. Efficiencies normally describe steady-state conditions. Efficiencie also reflect the overall losses in a system. Additional losses occur in nearly any of the energy conversion steps during dynamic conditions [101]

4.2 Metreological parameters analysis.

From the table7 it is observed that the distribution of of tilted radiation (G_T) along the day amounts to 5.051kW, the results matching with the design month(June) computations, shown by table 7 of radiation on tilted plane for Tosing $\pm 5^{\circ}$about latitude and figure 8 of the design month evaluation. Comparing the results of Hove and Mungofa [17] their design month(January) showed least tilt factor and least energy yield, there reason being high radiations received, yet in this case study latitudes of -30.36° the radiation is essepecially during winter periods. Proven by the results of mapped Lesotho beam radiation map from gridded data base developed for June month, illustrated by figure 19, showing low radiations of less than 4.0kW/m^2/hr.

The hourly time step variation of ambient temperatures of the system are shown on table 15 along the day, matching with the developed minimum temperature map. The maximum ambient temperature from figure 20, However of -1.0˚C calculated at mid hour (07:30hours), with the maximum efficiency of the PV module(η_{pv}) of 15.20%. At 06:30 hours the system had not reached threashold power needed to start pumping, that is insufficient radiation.

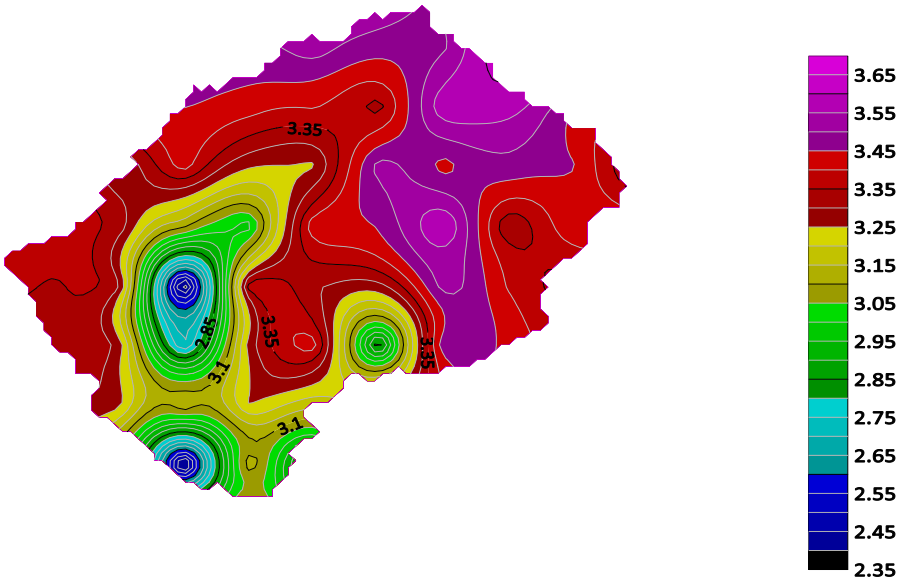

Figure 19 Lesotho beam radiation map developed for June month

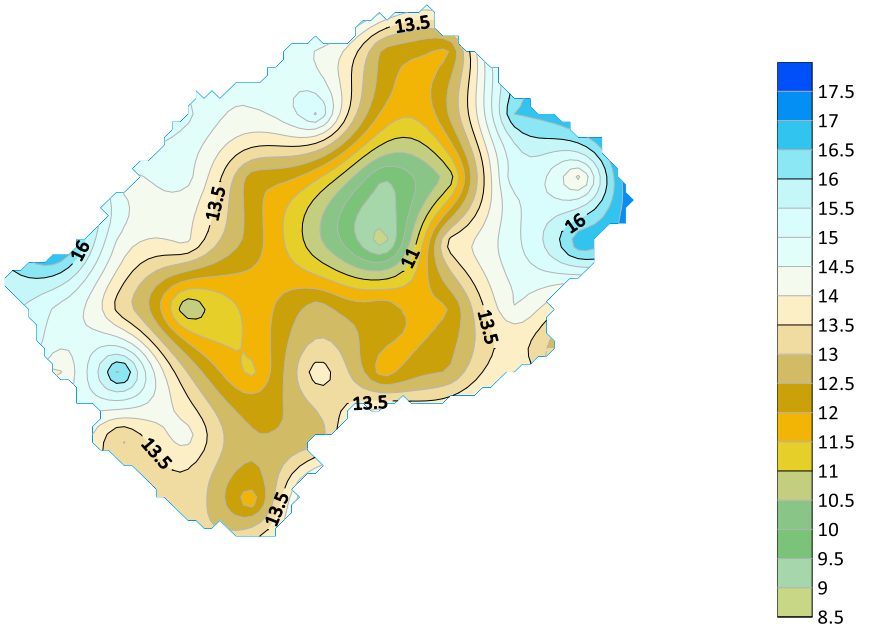

Figure 20 Lesotho maximum temperature map developed for June month

4.3 Designed Systems predictions and economic analysis.

The relation between PV array power and the flow rate is logarithmic and the PV array power required is parametric to the diameter of the pipe connected to the solar pump-pipe system is shown on Figure 14. The PV array power required decreases, as illustrated on figure 20; as the pipe diameter is increased.

All the systems of the sampled design pipes of specified diameters, are designed to deliver 350m3/day in June (the lowest producing month), their cost values are different, since they used different PV array and pipe sizes. Further, they deliver some different annual volumes of water as shown on Figure 21. As it can be observed that, November and December yield well over 600m^3/day, for this 140mm_ pipe design system. The required PV array power reduces significantly as the pipe diameter is increased from 125 mm to 200 mm. Although each of the systems is designed to deliver 350 m3/day in June (the least productive month), their cost structures are different, since they used different PV array and pipe sizes. Further, they deliver slightly different annual

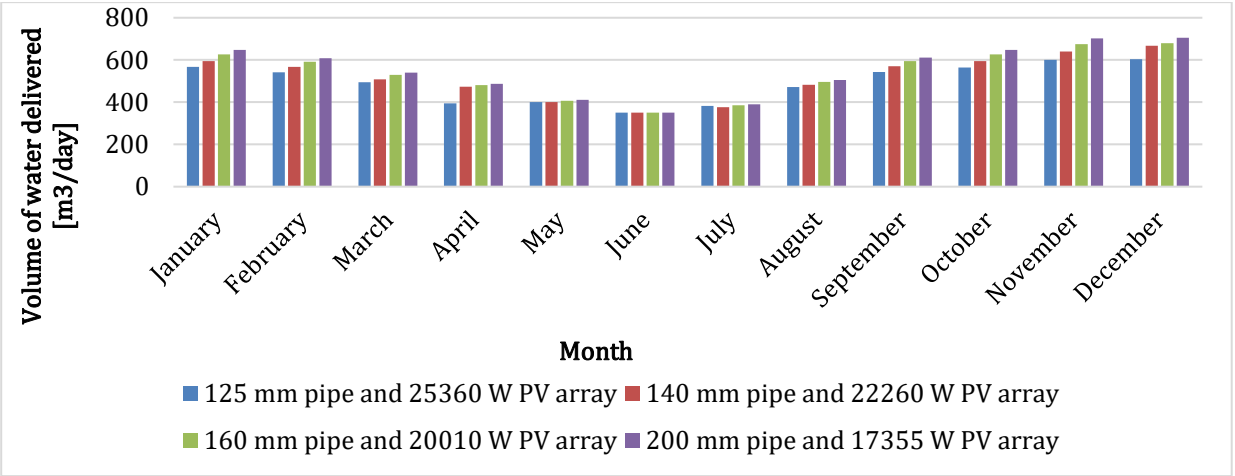

Figure 21 Monthly variation of daily-water delivery of all sampled pump-piping systems

For purpose of demonstrating the objective of this particular study; the comparison of the systems' cost effectiveness, of the least unit cost of pumping is compared. This is illustrated by of table 17, the system with the least unit cost of pumping, which is the needed system, the one that is connected a 140 mm diameter, with a pumping length 3000 and demanded 22260 Watts PV array. The unit cost of pumping for this system is $4.05 cents per cubic meter of water pumped for Tosing community. From volumes of water as shown on figure 22. The choice of the PV-pump-pipe design is not obvious since a larger diameter pipe (large pipe costs) requires a smaller PV array size (small PV array costs). In principle, the size of the pump itself may also vary for different pipe diameters used to perform a given pumping duty, therefore changing the cost structure of the PV-pump-pipe system this is clearly illustrated by figure 22.

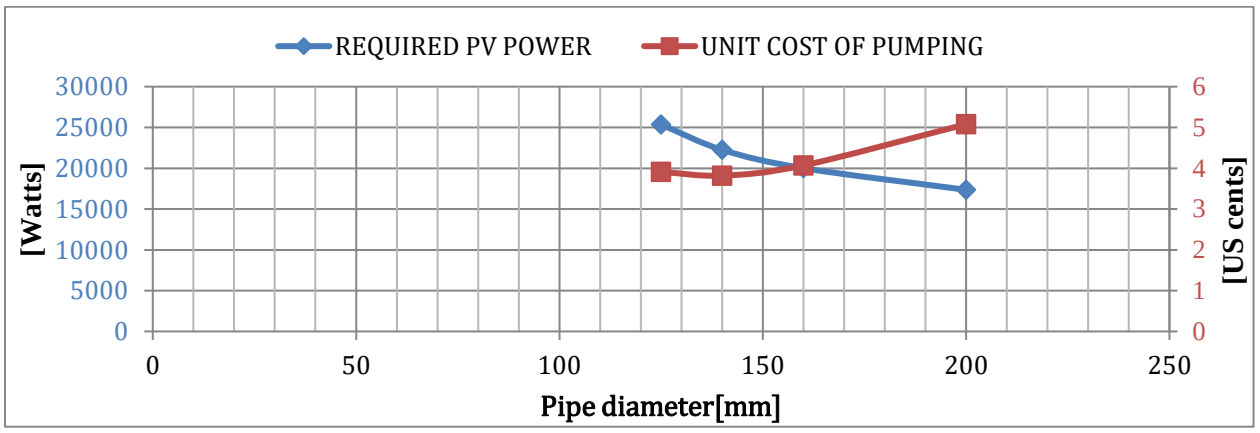

Figure 22 cost of pumping analysis

4.4 Case study method against traditional methods

To demonstrate the prominent advantage of the method applied, considering daily water demand 350 m3/day, the required pump flow rate is obtained by dividing the daily demand by the effective peak sunshine hours, for the month receiving the lowest tilted-radiation. From Table 6 and 7, the lowest tilted-plane irradiation is received for the month of June. The monthly average global horizontal irradiation is 3.29 kWh/m^2/day and the tilt factor is 1.505, resulting in global irradiation on the tilted plane of 5.051 kWh/m^2/day.

Some of this radiation is available above the critical irradiance for pump to operation. This fraction is estimated here to be 0.95. Therefore, the effective monthly average irradiation available for pump operation is 0.95 x 5.051, which is 4.798 kWh/m2/day ordinary 4.798 peak sunshine hours. Therefore, the required flow-rate of the pump is 350 m3 divided by 4.798 hours, equals about 73m3/hr. For the design pipe of 140 mm diameter is selected. From the computations of frictional losses in section I methodology section, the Hazen-Williams formula yields a frictional head loss of about 25 m for a flow-rate of 73m3/hr over a distance of 2000 m. Therefore, the total dynamic head for a static head of 60 m is 98m. From the selected pump characteristic curve, the nominal PV array power required to deliver 73m3/hr at 98 m head is 27.5 kW

This demonstrates that in the simple methods the pump efficiency is maximized to higher frequency thus requiring higher power. This leads to oversized systems because morning hours and late afternoon input of power is ignored. Also efficiency of PV is compromised during peak hours leading to reduced overall efficiency. Now to analyse the difference with the PV array power calculated by this particular study method, a de-rating factor that includes both PV module mismatch factor and temperature de-rating, as done in equation 13, should be included in the analysis. A cell temperature of about 31.1˚C, which, for example in Table 15, is the peak cell temperature between 10:00hours and 14:00hours pm (when the largest amount of solar energy is produced), equation 13, yields a temperature de-rating factor, $\eta_{pv}/\eta_{ref}/$, of about 0.88.Therefore, the PV array power that would have been prescribed using the simple design method is 27.5/0.81 or 33.95 kW.

Compared with the PV array power prescribed by the study method (22.26 kW), the PV array size prescribed by the simple sizing method is 25% larger. The reason for this deviation is that the conventional sizing method uses a single average flow-rate calculated based on average peak sunshine hours, resulting in an overestimates of the total dynamic head, which is higher than the variable flow-rates and total dynamic head actually obtaining during pump operation.

Another difference is the balancing storage size, which can be calculated using hourly mass balance with the study method, but is assumed equal to daily water demand with the simplified method. As shown in methodology section, the storage capacity sized using the study method is 255m^3 of balancing storage capacity should be added 3to5 days to secure for system shutdowns. However still very small as compared to that obtained by the traditional sizing method where water demand of 350m^3/day is multiplied by estimates of outage of power days (3to5 days) [68].

Table 17 of study method results as compared to traditional

	Study method	Traditional methods	% DIFFERENCE (TRADITIONAL-/STUDY)
TDH		79 m	
Water output	350 m^3/day	471 m^3/day	34 %
Pv power required	22.26 Kw	28.0 kW	25.8 %
Cost of pumping	3.82 cents/ m^3	4.41 cents/m^3	14 %
9Storage size	255* day of autonomy	350* days of autonomy	37.3 %
Pipe diameter	140 mm	160 mm	14 %
Maximum Flow velocity	1.32 m/s	0.9 m/s	

Table 17 of study method results as compared to traditional The method proves to be a significant advantage over the traditional simplified approach of sizing solar pumping systems. It resulted in significantly reduced unit cost of pumping and reduced cost of storage. Table18 applied method trend of Zimbabwe and Lesotho clearly identify the critical parameters that makes different from the location where the method is already applied so that using this established method in different settings could provide some additions to the existing knowledge. Costs of PV equipment and water pumps are have decreased hence PV pumping systems more economic lately.

Table18 applied method trend of Zimbabwe and Lesotho

	Zimbabwe Longitude 27.46; Latitude -17.67	Lesotho Longitude 27.90, Latitude -30.36
Design moth	January	June
Radiation on tilted plane	5.859 kWh/m^2/day	5.051 kWh/m^2/day
Water demand	250 m^3/day	350 m^3/day
Pv power required	12.6kW	22.6kW
Design pipe	125mm	140mm
System overall efficiency	6.0	7.1
Cost of pumping	5.22US cents/m^3	3.82 US cents/m^3

CHAPTER 5 CONCLUSIONS AND RECOMMENDATIONS

5.1 Conclusions

Hove and Mungofa method of optimal sizing and prediction performance of a solar pumping system was demonstrated for a solar PV pumping system located in Lesotho. For a prescribed Lorentz PSk-2-40-C-SJ95-7 pump, the components of the solar pumping system that have to be precisely sized are the PV array, the pipe diameter and the storage tank. The method accounts holistically the instantaneous variations of solar irradiance with shorter (hourly) to longer periods (monthly), evaluated and its effect on the pump system flow-rate and total dynamic head. For a given pipeline diameter, the PV array power that can deliver a required daily volume of water, under the mentioned instantaneous variation of pump operating parameters, had be arrived at performing trial and error analysis.

The applied method is especially suitable for long pipelines, the PV array power required to deliver a specified daily volume of water lowers significantly as the pipe diameter is increased. Depending on the relative specific costs of PV array and pipe from suppliers and manufacturers, an economically optimum (least unit cost of pumping) combination of these two system components, which delivers the desired daily volume of water, have been achieved.

For this study undertaken for Tosing (-30.36° latitude 27.90° longitude) community; to supply of potable water of 350m^3/day, optimized system of 60 meters static head, 140mm pipe diameter and 3000m length connected to Lorentz PSk-2-40-C-SJ95-7 submersible solar pump, arrived at the following conclusions.

- The design month is June with optimum tilt angle of 35.36°. From global horizontal irradiation of 3.29kW/m^2/day the irradiation on collector is 5.051kW/m^2/day.
- Required PV array of 22.3 kW. Attaining the least unit cost of pumping of 3.82 US cents/m^3.
- Compared with simplified methods; which estimated required of PV array of 27.5 kW, 25 % larger than this study method.
- For designed system his study predicts maximum yield of over 600m^3/day for November and December months.
- Compared with simplified methods, this case study optimized the storage capacity to be 37 % less than the sizing of simplified methods.

Therefore applied method is a significant improvement to the commonly used simplified approach of sizing solar pumping systems as it can result in significantly reduced system size. Using this study method, it is also more possible to predict the monthly average hourly variation of delivered water as well as its month-to-month variation.

With knowledge of the average hourly variation of volume of water delivered coupled with information on the diurnal water demand, it is possible to more accurately estimate the required balancing water storage size for the solar pumping scheme, which turns out to be much smaller than the ordinarily assumed storage capacity.

Solar pumps can meet a wide range of needs and are relatively simple, reliable, cost competitive, and low maintenance costs. This thesis represents a first attempt at studying the suitability of PVWPS technology for access to clean affordable and reliable water and energy services, for supporting the sustainable development goals for rural communities in Lesotho. This study thus provides an overview on how to design, optimize, and assess the technical and economic feasibility of PVWP systems. The other contribution of the this study was to develop meteorological variables grid for specified study area of Lesotho, also the study constructed bilinear interpolation program to estimate meteorological parameters magnitudes at any location in Lesotho. The developed grid was mapped with surfer software.

Furthermore the study derived power-flow functions that directly relate the PV power to flowrate for specific pump-pipe sampled for this preset study. To establish hourly response functions as the system reacts to non-linear variations of the flowrate (pump-response) to system resistance as they are functions to solar PV electric output, which is it also the function variable meteorological factors. Hove and Mungofa model [17] was also applied to optimise and size the solar pumping system components using derived power flow functions and long term meteorological data , for hypothetical case study of 350m^3/day potable water supply for Tosing community (-30.36 latitude, 27.90 longitude), Lesotho.

The objective function of the least unit cost of pumping was attained, through sizing the system with combination of optimally efficient components. The study also applied the developed grid data base of long term monthly averages to predict hourly variations of optimised systems performance, from monthly to hourly time step variations, accurate predictions of water output for Tosing water supply scheme were evaluated.

The limitations of this study and the issues that require further investigation are disclosed in this paragraph. The meteorological data from another source different that the one PVGIS-CAMSAF and NASA provided can give some differences about the real measures. In this case, the data source is from PVGIS and NASA and not from any meteorological station located in the surroundings of the site. Therefore for this particular thesis the applied data may not match perfectly with the real site data, the ground data from site of study was not available to apply. However it was not mandate of this study to validate data. Another limitation is the simulations carried out through Hove and Mungofa model may be slightly different from the ones that could be obtain in the reality due to limitations of the program, and certain approximations within it. Area of this

study that require further research is comparative assessment of different energy sources such as diesel generators , conventional grid or other renewable energy sources applied to water pumping system. Lesotho scenario of PVWPS requires also social based research to assess the up-taking of these technologies.

5.2 Recommendations

This paper would be useful for the researchers, engineers, manufacturers, and policy makers and may be a guide for efficient installation and performance enhancement of solar photovoltaic water pumping system. For this particular case study, as strategy for climate change drought emergency response program, for reliable, affordable, efficient energy and water services; department of rural water supply, Lesotho (DWRS) and department of energy (DoE) Lesotho are recommended specifically to adopt this model as part of rural electrification and rural water supply for its results of accuracy and economic advantages from the following direct impacts of the model.

- The model guides the selection of a proper solar_pump_pipe and storage; an optimum system parameter search can greatly enhance the performance of a PV pumping system to achieve the required water demand for living in a remote area.
- A well-designed PV pumping system is feasible in the Lesotho climate, the economic feasibility is based on certain assumptions, and the results of the comparison between PV pumping systems and conventional pumping systems will be influenced by changes in any of the key assumptions used, like period of analysis and reliability of the equipment for that period.
- The model with its interpolation program is especially suitable for the widespread implementation of these technologies across the whole country. Furthermore a technological improvement of model is recommended. Computer Programming can be used to upgrade the model to software application that is automated for easier application.

Lesotho policies (for example water, energy, climate, agriculture) seeking to promote this technology need to account for the direct and indirect impacts caused by solar energy technologies within the water-energy-food nexus. Particularly Lesotho government policies and regulations are required to promote the use of PV water pumps. When solar PV water pump system technologies are applied to reduce poverty, governments and international development agencies should reconsider their subsidies and support PVWPS programs. This study further recommend the need for greater social and institutional input in solar PV technologies especially when applied to water pumping systems for rural development and in particular to revisit institutional policy instruments and institution for technical assistance, training and credit services that will facilitate widespread implementations of solar water pumping systems in Lesotho. Most importantly, users should be trained on the economic use of water and how to preserve it for sustainable developments.

REFRENCECES

[1] WORLD BANK, "Directions in Development, Re-engaging in Agricultural Water Management: Challenges and Options," Washington, DC.U.S.A, 2006.

[2] Ramos J. S, Ramos H. M, "Solar powered pumps to supply water for rural or isolated zones: a case study," *Energy Sust Dev*, vol.13, pp.151–158, 2009.

[3] BUREAU OF STATISTICS, 2016. Maseru. Lesotho.

[4] UN STATISTICS REPORT,"World economic and social survey on sustainable development''. Available online at: www: //http UN Org. un pub/2843 E/2013/50/Rev/ST/ls/344. 2003. [Accessed 20/9/2019].

[5] GOVERNMENT OF LESOTHO, "Strategies for poverty," 2005. . Available online at: www: GOL Accessed 20/11/2019

[6] GOL, Ministry of Water Affairs Commissioner of Waters, Long-Term Water and Sanitation Strategy Volume II Water Sector Programme May 2014

[7] Department of Energy, "National Investment Policy of Lesotho," Government of Lesotho, Lesotho, 2016

[8] Y.G, Hailu, "Measuring and monitoring energy access: decision-support tools for policymakers in Africa," *Energy Policy*, vol. 47 (Suppl. 1), S56–S63, May. 2012.

[9] B. M. Taele, K. K. Gopinathan, and L. Mokhuts'oane, "The potential of renewable energy technologies for rural development in Lesotho," *Renew. Energy*, vol. 32, no. 4, pp. 609–622, Apr. 2007.

[10] I.Odeh, Y.G. Yohanis, B. Norton, "Economic viability of photovoltaic water pumping systems," *Sol Energy* , vol 80: pp. 850–860, July. 2005

[11] V.C. Sontake, V.R. Kalamkar, "Solar photovoltaic water pumping system:-A comprehensive review," *Renew. Sustain. Energy Rev.*, vol. 59 pp.1038–1067, June 2016.

[12] N. Hamrouni, M. Jraidi, A. Chérif, "Solar radiation and ambient temperature effects on the performances of a PV pumping system," *Rev. Energy. Renewables*, vol 11 (1) PP 95–106. 2006.

[13] M. Mpholo *et al.*, "Rural Household Electrification in Lesotho," in *Africa-EU Renewable Energy Research and Innovation Symposium 2018 (RERIS 2018)*, 2018, pp. 97–103.

[14] Hobbs GW, Morrison GL. "Solar photovoltaic water pumping system design and performance," In: *Proc. Solar'86-at work in the community*, 1986. p. 298 -307.

[15] M. Jafar, J. Roberts, C. Narayan,"Small-scale solar water pumping in Fiji: performance testing of the Solar Star 1000 solar water pump," *Report prepared for Dept. of Energy (Fiji).*1996.

[16] S. Eyad, S. Al-Soud, "Potential of solar energy development for water pumping in Jordan," *Renew Energy*, vol.29:pp.1393–1399.2004.

[17] T.Hove, E. Mungofa, "Towards the optimal sizing of solar-powered pump-pipe-storage systems." in *Africa-EU Renewable Energy Research and Innovation Symposium 2018 (RERIS 2018)*, 2018, pp. 45-58.

[18] Ruiz B.E, "Design of a PV-system with batteries connected building for a grid," Master's thesis, in energy Systems. University of Gavel, Sweden. 2017.

[19] European Commission, "Best practices on Renewable Energy Self-Consumption," Brussels, 2015.

[20] G. Boyle,"Renewable Energy - Power for a sustainable future", Oxford University Press, UK. 2012.

[21] W. Witzel and D. Seifried' "Renewable Energy - The Facts", Energieagentur, Freiburg, Germany. 2010.

[22] Duffie JA, Beckman WA. In: Solar engineering of thermal processes. 2nd edition. New York: John Wiley & Sons; p. 39 -43. 1991.

[23] M. De Felice, "Scoping the potential usefulness of seasonal climate forecasts for solar power management," Renewable Energy vol142, pp215-223, 2019.

[24] Cano .D et al, "A method for the determination of the global solar radiation from meteorological satellite data". Solar Energy 37, 31‐39. 1986.

[26]T. Huld, R. Muller, A. Gambardella, "A new solar radiation database for estimating PV performance in Europe and Africa." Solar Energy vol 86, pp 1803–1815. 2012.

[27] Collares-Pereira M, Rabl A. The average distribution of solar radiation- correlations between diffuse and hemispherical and between daily and hourly insolation values. *Sol Energy*; vol 22: pp155-64. 1979.

[28] Hove. T, Göttsche. J, "Mapping global, diffuse and beam radiation over Zimbabwe. Renew Energy; vol 18:pp535-56. 1999.

[29] Klein S.A, "Calculation of monthly average insolation on tilted surfaces." *Solar Energy*; vol 19:pp325-9.

[30] Kaldellis. J.K, Meidanis. E, Zafirakis. D "Experimental energy analysis of a stand-alone photovoltaic-based water pumping installation," Applied Energy vol 88, p4556–4562, 2011.

[32] Mansur, A et al, "Review of solar-powered water pumping systems," *Renewable and Sustainable Energy Reviews* vol 87 pp. 61–76. 2018.

[33] Chandel, S. et al, "Review of solar photovoltaic water pumping system technology for irrigation and community drinking water supplies," *Renewable and Sustainable Energy Reviews*, Volume 49, 1084-1099. 2015.

[34] Campana. P. E, Li. H, Yan. J. Dynamic modeling of a PV pumping system with special consideration on water demand. *Applied Energy* vol; 112: pp635‐45. 2013.

[35] Firatoglu. Z, Yesilata. B, "New approaches on the optimization of directly coupled PV pumping systems." *Solar Energy* vol77, pp 81‐93.2004.

[36] Short. T, Oldach. R, "Solar powered water pumps: the past the present and the future." *Journal of Solar Energy Engineering* vol25, pp76-82. 2003.

[37] Zaki, A., Eskander, M, "Matching of photovoltaic motor-pump systems for maximum efficiency operation." *Renewable Energy* vol 7(3), pp279-288.

[38] Barlow. R et al, "Solar pumping: an introduction and update on the technology, performance, costs and economics." World Bank Technical Paper No. 168. Intermediate Technology Publications and the World Bank, Washington, DC, USA. 1993.

[39] Benlarbi. K et al, "A fuzzy global efficiency optimization of a photovoltaic water pumping system. *Solar Energy* 77, 203–216.2004.

[40] Odeh. I, "Influence of pumping head, insolation and PV array size on PV water pumping system performance." Solar Energy, Volume 80, Issue 1, pp51-64.2004.

[41] Posorski. R, "Photovoltaic water pumps an attractive tool for rural drinking water supply." *Solar Energy* vol 58 (4-6), pp155-163. 1996.

[42] Eckstein .J.H, "Detailed modeling of photovoltaic system components." MS thesis. Mechanical Engineering, University of Wisconsin, Madison, 1990.

[43] Morshed .H, Abdulsalam. A, "Assessment of factors influencing the sustainable performance of photovoltaic water pumping systems." *Renewable and Sustainable Energy Reviews;* vol 92, pp 307–318.2018.

[44] Rawat. R, Kaushik. SC, Lamba. R, 'A review on modeling, design methodology and size optimization of photovoltaic based water pumping, standalone and grid connected system," *Renew Sustain Energy Rev* 2016; 57:1506–19. http://dx.doi.org/10.1016/j.rser.2015.12.228

[45] Jafar. M, "A model for small-scale photovoltaic solar water pumping." *Renewable Energy* 19, 85-90.2000.

[46] Jafar. M, "Small-scale solar water pumping in Fiji: performance testing of the solar star 1000 solar water pump." Unpublished Report. Fiji Department of Energy. 1996.

[47] Langridge. W, Lawrance.W, Wichert, B, "Development of a photovoltaic pumping system using a brushless DC motor and helical rotor pump." *Solar Energy*: vol56, pp151-160. 1996.

[48] Kou. Q, Klein. S, Beckman.W, "A method for estimating the long term performance of direct-coupled PV pumping systems." *Solar Energy*: vol 64, 33-40. 1998. [30] 2006; 47:2092–102.

[49] Al-Ibrahim A. M. Optimal selection of direct-coupled photovoltaic pumping system in solar domestic hot water systems PhD thesis. Madison, USA: Mechanical Engineering, University of Wisconsin; 1996.

[50] Klein S. A. In: TRNSYS user's manual, version 14.1. Madison, USA: Engineering Experimental Station, University of Wisconsin; pp. 2424–35. 1994.

[51] Badescu V. Time dependent model of a complex PV water pumping system. *Renewable Energy*; vol 28(4):543–60. 2003.

[52] Hadj Arab. A et al, "Motor-pump system modelization." *Renewable Energy*; vol 31(7): pp 905–13. 2006.

[53] Benghanem. M et al, "Estimation of daily flow rate of photovoltaic water pumping systems using solar radiation data," *Results in Physics*, Volume 8, pp 949-954. 2018.

[54] Abella MA, Lorenzo E, Chenlo F. PV water pumping systems based on standard frequency converters. Prog Photovoltaic: Res Appl; 11:179–91. 2003.

[55] Gao. Z, et al, "Progress on solar photovoltaic pumping irrigation technology," Irrig Drain; vol67:pp89–96. 2018.

[56] Hamidat. A, Benyoucef. B, "Mathematic models of photovoltaic motor-pump systems," Renewable Energy, Volume 33: pp 933–944, 2008.

[57] Chilundo. R, et al "Design and Performance of Photovoltaic Water Pumping Systems: Comprehensive Review towards a Renewable Strategy for Mozambique." *Journal of Power and Energy Engineering*; vol 6, pp32-63. 2018.

[58] PVSYST (2017). Available online at: http://www.pvsyst.com/en/

[59] HOMER (2017). Available online at: http://www.homerenergy.com/

[60] Retscreen (2017). Available online at: http://www.nrcan.gc.ca/energy/software-tools/7465

[61] SAM (2017). Available online at: https://sam.nrel.gov/

[62] MATLAB (2017). Available online at: https://www.mathworks.com.

[63] TRANSYS (2017). Available online at: https://sel.me.wisc.edu/trnsys/

[64] Lab VIEW (2016). Available online at: http://www.ni.com/pt-pt/shop/labview

[65] T. Hove, "A method for predicting long-term average performance of photovoltaic systems." *Renewable Energy*; vol 21 pp207-229.2000.

[66] Ghoneim AA. Design optimization of photovoltaic powered water pumping systems. *Energy Convers Manag*; vol47 (11–12):pp1449–63. 2006.

[67] Young .C ,"Plots, Curve-Fitting, and Data Modeling in Microsoft Excel." *Electrical Circuits and Systems*. 2009.

[68] Khatib.T, "Design of Photovoltaic Water Pumping Systems at Minimum Cost for Palestine: A Review. *Journal of Applied Sciences*, vol 10(22), pp.2773-2784. 2010.

[69] Loxsom, F, Durongkaveroj. P, "Estimating the Performance of a Photovoltaic Pumping System. *Solar Energy,* 52, pp215-219. 1994.

[70] Lorentz pumps," Available online at: Lorentz partnernet.com: accessed [12.12.19]

[71] Igor. J.P.M, Karassik. J, Cooper, P. and Heald.C.C, "Affinity laws," Pump Handbook. 4th Edition, McGraw-Hill, New York.

[72] Walski, T. M. "A history of water distribution", Journal-American Water Works Association, 98 (3): 110–121, p. 112.March, 2006.

[73] WAGDY R. ANIS and M. A. NOURZ, "optimum design of a photovoltaic powered pumping system," *Energy Conversion. Management* Vol. 35, No. 12, pp. 1123 -1130. 1994

[74] T. Hove, E. Manyumbu, G. Rukweza, " Developing an improved global solar radiation map for Zimbabwe through correlating long-term ground- and satellite-based monthly clearness index values," *Renewable Energy* vol 63 pp687-697, 2014.

34[75] Khan MTA, Ahmed MR, Ahmed SI, Khan, "Design and Performance analysis of water pumping using solar PV," *In: Proceedings of the international conference of developments in renewable energy technology* (ICDRET). 2012.

[76] Bakelli. Y, Hadj, A. and Azoui, C,"Optimal sizing of photovoltaic pumping system with water tank storage using LPSP concept," *Solar Energy*, Volume 85, Issue 2, 288-294.

[77] Morshed. H, Abdulsalam. A, "Assessment of factors influencing the sustainable performance of photovoltaic water pumping systems," *Renewable and Sustainable Energy Reviews* vol-92 pp 307–318, 2018.

[78] Surfer software 16, "Contouring and 3D surface mapping software. Available online at: www.ssg-surfer.com. [Accessed 12.12.19]

[79] Zelenka, A et al, "Effective accuracy of satellite-derived hourly irradiances" *Theor. Applied. Climatololgy*. 62, 199–207.1999

[80] Su'ri, M., Huld, T., Dunlop, E.D., 2005. PV-GIS: a web-based solar radiation database for the calculation of PV potential in Europe. J. *Sustain. Energy*. 24, 55–67

[81] Soda, Available online at: SoDa (http://www.soda-is.com),

[82] Satel-light, Available online at: Satel-Light (http://www.satellight.org),

[83] NASA SSE Available online at: NASA SSE (http://eosweb.larc.nasa.gov/sse/).

[84] NREL, Available online at: NREL (http://rredc.nrel.gov/solar).

[85] Wikipedia, "Bilinear 2 dimensional illustration," Available on: http://en.wikipedia.org/wiki/. Bilinear Interpolation [accessed on 04.11.19].

[86] William H; Teukolsky, Saul A.; Vetterling, William T; Flannery, Brian P. (1992). Available online at: *Numerical recipes in C: the art of scientific computing* (2nd ed.). New York, NY, USA: Cambridge University Press. pp. 123-128. [Accessed 15.2.20]

[87] H. P. Garp, G. L. Gupta. "Solar photovoltaic applications,'' In: *Proceedings of the International Solar Energy Society, Congress* 1134, and New Delhi 1978.

[88] M. Iqbal, Optimum collector slope for residential heating in adverse climates. *Solar Energy* VOL: 22 pp77−9.1979.

[89] T. Pavlović, Z. Pavlović, L. Pantić, Lj. Kostić, "Determining optimum tilt angles and orientations of photovoltaic panels in Niš, Serbia" *Original scientific papers UDK* 694:547.281:66.094 DOI: 10.5767/anurs.cmat.100102.en.151P. Contemporary Materials I−2 (2010)

[90] Lewis G, 'Optimum tilt of solar collectors." *Solar and Wind Technology* 4 (1987) 407.

[91] Almeidaa. R. H, Ledesmaa. J. R, Carrêloa. I. B,Narvartea. L, Ferrarac. G, L. Antipodic. L, "A new pump selection method for large-power PV irrigation systems at a variable frequency *Energy Conversion and Management* 174 (2018) 874–885

[92] Argaw. N,"Optimal load matching in photovoltaic water pumps coupled with DC/AC inverter,"

International Journal of Solar Energy 18, 41–52. 1995.

[93] Hazen- William Frictional losses calculator, available online at: https://goodcalculators

[Accessed 15.12.12].

[94] DPI Plastics (Pty) Ltd, manufacturer of PVC and HDPE water reticulation and drainage pipe and fitting systems SABS or international ISO-9001 certified, available online at: https://dpi plastics.com. Johannesburg, SA. 2018. [Accessed 15.01.20].

[95] Brandumahel. M. J, Beckman, W. A, "Economic evaluation and optimization of solar heating systems," *Solar Energy* 1979; 23:1–10.

[96] Solar module prices: available online at: https:www.enfsolar.com; [accessed 15.01.20].

[97] Pump prices: Available online at: https://www.alibaba.com ; [accessed 15.01.20].

[98] Pipe prices: Available online at: http://www.kuzeyboru.com; [accessed 15.01.20].

[99] Blokker, M, Stochastic water demand modelling, London: IWA Pub., pp. 37. available online at:. https://www.drink-water-eng-sci.net. dwes-10-1-2017.xml10/1/2017 · SIMDEUM . [accessed 25.01.20].

[100]Boutelhig. A, Hanini. S, Arab, A. H,"Performances' investigation of different photovoltaic water pumping system configurations for proper matching the optimal location, in desert area," *Energy Convers Manage* ;pp 151:439–56. 2017.

[101] Bucher W. Aspects of solar water pumping in remote regions. *Energy Sust Development* ;3: pp 8–27.1996.

ANNEXES

Pipe diameters: Southern African a standards

Outside Dia.mm	Class 6		Class 9		Class 12		Class 16		Class 20		Class 25	
	mm	kg	mm	kg	mm	kg	mm	kg	mm	kg	mm	kg
50	1.5	2.1	1.5	2.1	1.7	2.4	2.2	3.0	2.7	3.7	3.3	4.4
63	1.5	2.7	1.6	2.8	2.1	3.7	2.7	4.7	3.4	6.0	4.1	7.0
75	1.5	3.2	1.9	4.0	2.5	5.3	3.2	6.8	4.0	8.2	4.9	10.0
90	1.8	4.6	2.2	5.6	3.0	7.6	3.9	9.7	4.8	11.9	5.9	14.4
110	2.2	6.9	2.7	8.4	3.6	11.1	4.7	14.4	5.8	17.6	7.2	21.5
122	-	-	-	-	4.0	13.3	5.2	17.2	-	-	-	-
125	2.5	8.9	3.1	11.0	4.1	14.4	5.4	19.1	6.6	22.7	8.2	27.9
140	2.8	11.2	3.5	14.2	4.6	18.1	6.0	24.1	7.4	28.6	9.1	35.8
160	3.2	14.6	4.0	18.2	5.2	23.5	6.9	30.8	8.5	37.6	10.4	45.5
177	-	-	-	-	5.8	28.1	7.7	36.8	-	-	-	-
200	3.9	22.3	4.9	27.9	6.5	36.8	8.6	48.2	10.6	60.3	13.0	71.3
250	4.9	35.1	6.1	44.9	8.1	57.6	10.7	75.4	13.2	94.6	16.3	112.5
315	6.2	56.3	7.7	69.7	10.2	91.7	13.5	120.3	16.6	146.7	-	-
355	7.0	72.0	8.7	89.2	11.5	117.3	15.2	153.6	-	-	-	-
400	7.8	90.3	9.8	113.5	13.0	149.8	17.1	195.4	-	-	-	-
450	8.9	116.7	11.0	144.0	14.6	190.1	-	-	-	-	-	-
500	9.8	144.4	12.2	177.7	16.2	234.8	-	-	-	-	-	-
560	11.0	182	13.5	222	17.1	280	23.4	378	-	-	-	-
630	12.5	232	15.4	285	20.4	375	26.9	489	-	-	-	-

Source: DPI Plastics (Pty) Ltd

Pipe prices ad pressure codes

OD MM	CODE	PN4 MT/USD	CODE	PN6 MT/USD	CODE	PN10 MT/USD	CODE	PN16 MT/USD
20	-	-	-	-	-	-	1.4.02016	0,35
25	-	-	-	-	-	-	1.4.02516	0,62
32	-	-			1.4.03210	0,70	1.4.03216	0,97
40	-	-			1.4.04010	0,95	1.4.04016	1,38
50	-	-	1.4.05006	1,11	1.4.05010	1,46	1.4.05016	2,16
63	-	-	1.4.06306	1,51	1.4.06310	2,27	1.4.06316	3,43
75	1.4.07504	1,73	1.4.07506	2,05	1.4.07510	3,24	1.4.07516	4,86
90	1.4.09004	2,38	1.4.09006	3,00	1.4.09010	4,64	1.4.09016	6,80
110	1.4.11004	3,08	1.4.11006	3,56	1.4.11010	5,67	1.4.11016	8,59
125	1.4.12504	3,97	1.4.12506	4,62	1.4.12510	7,29	1.4.12516	10,96
140	1.4.14004	5,59	1.4.14006	5,81	1.4.14010	9,18	1.4.14016	13,64
160	1.4.16004	6,48	1.4.16006	7,56	1.4.16010	12,02	1.4.16016	17,82
200	1.4.20004	9,75	1.4.20006	11,75	1.4.20010	18,63	1.4.20016	27,81
225	1.4.22504	12,42	1.4.22506	14,85	1.4.22510	23,44	1.4.22516	35,37
250	1.4.25004	15,26	1.4.25006	18,09	1.4.25010	28,89	1.4.25016	43,20
280	1.4.28004	19,20	1.4.28006	22,82	1.4.28010	36,45	1.4.28016	54,54
315	1.4.31504	24,35	1.4.31506	28,62	1.4.31510	45,09	1.4.31516	69,12
355	1.4.35504	30,78	1.4.35506	36,72	1.4.35510	57,24	1.4.35516	87,75
400	1.4.40004	39,15	1.4.40006	46,17	1.4.40010	72,36	1.4.40016	110,70

Source: **Kuzeyboru**

PVC fittings prices

KAYARMANŞON		
PVC COUPLER		
OD MM	CODE	PCS/USD
50	1.24.05016	0,70
63	1.24.06316	1,18
75	1.24.07516	1,83
90	1.24.09016	2,83
110	1.24.11016	3,69
125	1.24.12516	5,19
140	1.24.14016	6,59
160	1.24.16016	9,21
200	1.24.20016	16,80
225	1.24.22516	21,99
250	1.24.25016	32,28
280	1.24.28016	43,43
315	1.24.31516	57,29
355	1.24.35516	93,68
400	1.24.40016	134,71

Source: Kuzeyboru

ANNEX 3

Pump technical sheet.

Solar Submersible Pump System

System Overview

Head	max. 110 m
Flow rate	max. 119 m³/h

Technical Data

Controller PSk2-40

- High efficiency solar pump controller
- Hybrid power (solar / grid / generator) support with LORENTZ SmartSolution
- Inputs for water meter, pressure sensors, digital switches
- Simple configuration with LORENTZ PumpScanner Android™ App
- Onboard data logging and system monitoring
- Inbuilt applications for constant pressure, constant flow and daily amount
- Integrated Sun Sensor
- Active temperature management
- Integrated MPPT (Maximum Power Point Tracking)

Power	max. 37 kW
Input voltage	max. 850 V
Optimum Vmp**	> 575 V
Motor current	max. 65 A
Efficiency	max. 98 %
Ambient temp.	-30...50 °C
Enclosure class	IP54

Motor AC DRIVE SUB 6" 30kW

- Highly efficient 3-phase AC motor
- Frequency: 25...52 Hz
- Premium materials, stainless steel: AISI 304
- No electronics in the motor

Motor speed	1 400...2 965 rpm
Power factor	0,88
Insulation class	F
Enclosure class	IP68
Submersion	max. 300 m

ANNEX 3

Solar PV technical data:

Electrical data

Nominal Power Watt Pmax(Wp)	295Wp	300Wp	305Wp	310Wp	315Wp
Power Output Tolerance Pmax(W)	0/+5	0/+5	0/+5	0/+5	0/+5
Maximum Power Voltage Vmp(V)	36.34V	36.59V	37.02V	37.31V	37.64V
Maximum Power Current Imp(A)	8.12A	8.2A	8.24A	8.31A	8.37A
Open Circuit Voltage Voc(V)	45.5V	45.6V	45.7V	45.81V	45.91V
Short Circuit Current Ioc(A)	8.7A	8.78A	8.82A	8.87A	8.94A
Module Efficiency m(%)	15.25%	15.50%	15.76%	16.02%	16.28%
Maximum system voltage	1000V				
Operating temperature	-40℃ to+85℃				
NOCT	45℃ to ± 2℃				
Temperature coefficient of Isc	+0.05%/ ℃				
Temperature coefficient of Voc	-0.34%/ ℃				
Temperature coefficient of Pm	-0.42%/ ℃				

Specifications included in this datasheet are subject to change without prior notice

ANNEX 4:

Simulations results for different pipes:

125mm results performance table for June

TIME		G	Ta	Tc	ηPV/ηREF	Ppv	Qop [m3/h	THD	ρgQopTDHo	ηpump	ηover	ηpv
05:00-06:00												
06:00-07:00	6.5	0	-0.4	-0.4	0.99	0	0.000	60.0	0	0.0%	0.0%	0.00%
07:00-08:00	7.5	152	-1.0	3.2	0.98	3316	4.456	60.2	730	22.0%	3.3%	15.20%
08:00-09:00	8.5	324	-0.3	8.6	0.96	6927	29.043	62.4	4940	71.3%	10.6%	14.89%
09:00-10:00	9.5	494	1.6	15.2	0.94	10293	42.265	64.6	7444	72.3%	10.5%	14.51%
10:00-11:00	10.5	630	4.3	21.6	0.91	12797	49.532	66.1	8928	69.8%	9.9%	14.15%
11:00-1200	11.5	706	7.3	26.6	0.89	14041	52.629	66.9	9588	68.3%	9.5%	13.86%
12:00-13:00	12.5	706	9.9	29.3	0.88	13886	52.259	66.8	9508	68.5%	9.4%	13.70%
13:00-14:00	13.5	630	11.8	29.1	0.88	12410	48.507	65.9	8713	70.2%	9.6%	13.72%
14:00-15:00	14.5	494	12.4	26.0	0.90	9854	40.810	64.4	7156	72.6%	10.1%	13.89%
15:00-16:00	15.5	324	11.8	20.7	0.92	6606	27.462	62.2	4654	70.5%	10.0%	14.20%
16:00-17:00	16.5	152	9.9	14.1	0.94	3180	3.058	60.1	501	15.7%	2.3%	14.57%
17:00-18:00	17.5	0	7.3	7.3	0.97	0	0.000	60.0	0	0.0%	0.0%	0.00%
TOTAL VOLUME		**4611**	**6.2**	**16.8**	**0.93**	**95487**	**350.0**	**63.29**	**62162**	**0.50**	**7.1%**	

140mmPerfomance table for June

TIME		G	Ta	Tc	ηPV/ηREF	Ppv	Qop [m3/h	THD	ρgQopTDHo	ηpump	ηover	ηpv
05:00-06:00												
06:00-07:00	6.5	0	-0.4	-0.4	0.99	0	0.000	60.0	0	0.0%	0.0%	0.00%
07:00-08:00	7.5	152	-1.0	3.2	0.98	3480	9.093	61.6	1527	43.9%	6.7%	15.20%
08:00-09:00	8.5	324	-0.3	8.6	0.96	7269	29.947	72.3	5897	81.1%	12.1%	14.89%
09:00-10:00	9.5	494	1.6	15.2	0.94	10802	41.160	81.9	9189	85.1%	12.3%	14.51%
10:00-11:00	10.5	630	4.3	21.6	0.91	13429	47.323	88.4	11402	84.9%	12.0%	14.15%
11:00-1200	11.5	706	7.3	26.6	0.89	14735	49.950	91.4	12446	84.5%	11.7%	13.86%
12:00-13:00	12.5	706	9.9	29.3	0.88	14572	49.636	91.1	12318	84.5%	11.6%	13.70%
13:00-14:00	13.5	630	11.8	29.1	0.88	13023	46.454	87.5	11070	85.0%	11.7%	13.72%
14:00-15:00	14.5	494	12.4	26.0	0.90	10341	39.926	80.7	8783	84.9%	11.8%	13.89%
15:00-16:00	15.5	324	11.8	20.7	0.92	6933	28.605	71.3	5557	80.2%	11.4%	14.20%
16:00-17:00	16.5	152	9.9	14.1	0.94	3337	7.908	61.3	1321	39.6%	5.8%	14.57%
17:00-18:00	17.5	0	7.3	7.3	0.97	0	0.000	60.0	0	0.0%	0.0%	0.00%
TOTAL VOLUME		**4611**	**6.2**	**16.8**	**0.93**	**100206**	**350.0**	**75.63**	**79512**	**0.63**	**8.9%**	

160mm Performance table for June

TIME		G	Ta	Tc	ηPV/ηREF	Ppv	Qop [m3/h	THD	ρgQopTDHo	ηpump	ηover	ηpv
05:00-06:00												
06:00-07:00	6.5	0	-0.4	-0.4	0.99	0	0.000	60.0	0	0.0%	0.0%	0.00%
07:00-08:00	7.5	152	-1.0	3.2	0.98	3130	0.000	60.0	0	0.0%	0.0%	15.20%
08:00-09:00	8.5	324	-0.3	8.6	0.96	6538	27.924	63.6	4842	74.1%	11.0%	14.89%
09:00-10:00	9.5	494	1.6	15.2	0.94	9715	43.122	67.7	7957	81.9%	11.9%	14.51%
10:00-11:00	10.5	630	4.3	21.6	0.91	12078	51.475	70.6	9902	82.0%	11.6%	14.15%
11:00-1200	11.5	706	7.3	26.6	0.89	13252	55.035	71.9	10790	81.4%	11.3%	13.86%
12:00-13:00	12.5	706	9.9	29.3	0.88	13106	54.610	71.8	10682	81.5%	11.2%	13.70%
13:00-14:00	13.5	630	11.8	29.1	0.88	11713	50.297	70.2	9616	82.1%	11.3%	13.72%
14:00-15:00	14.5	494	12.4	26.0	0.90	9301	41.449	67.2	7590	81.6%	11.3%	13.89%
15:00-16:00	15.5	324	11.8	20.7	0.92	6235	26.106	63.3	4500	72.2%	10.2%	14.20%
16:00-17:00	16.5	152	9.9	14.1	0.94	3002	0.000	60.0	0	0.0%	0.0%	14.57%
17:00-18:00	17.5	0	7.3	7.3	0.97	0	0.000	60.0	0	0.0%	0.0%	0.00%
TOTAL VOLUME		**4611**	**6.2**	**16.8**	**0.93**	**90125**	**350.0**	**65.52**	**65879**	**0.53**	**7.5%**	

200mm Performance table for June

TIME		G	Ta	Tc	ηPV/ηREF	Ppv	Qop [m3/h	THD	ρgQopTDHo	ηpump	ηover	ηpv
05:00-06:00												
06:00-07:00	6.5	0	-0.4	-0.4	0.99	0	0.000	60.0	0	0.0%	0.0%	0.00%
07:00-08:00	7.5	152	-1.0	3.2	0.98	3076	0.000	60.0	0	0.0%	0.0%	15.20%
08:00-09:00	8.5	324	-0.3	8.6	0.96	6426	24.281	69.5	4599	71.6%	10.7%	14.89%
09:00-10:00	9.5	494	1.6	15.2	0.94	9549	42.993	85.4	10000	104.7%	15.2%	14.51%
10:00-11:00	10.5	630	4.3	21.6	0.91	11871	53.278	97.2	14116	118.9%	16.8%	14.15%
11:00-1200	11.5	706	7.3	26.6	0.89	13025	57.660	103.0	16179	124.2%	17.2%	13.86%
12:00-13:00	12.5	706	9.9	29.3	0.88	12882	57.137	102.3	15922	123.6%	16.9%	13.70%
13:00-14:00	13.5	630	11.8	29.1	0.88	11512	51.827	95.4	13475	117.1%	16.1%	13.72%
14:00-15:00	14.5	494	12.4	26.0	0.90	9141	40.933	83.2	9285	101.6%	14.1%	13.89%
15:00-16:00	15.5	324	11.8	20.7	0.92	6128	22.043	68.1	4091	66.8%	9.5%	14.20%
16:00-17:00	16.5	152	9.9	14.1	0.94	2950	0.000	60.0	0	0.0%	0.0%	14.57%
17:00-18:00	17.5	0	7.3	7.3	0.97	0	0.000	60.0	0	0.0%	0.0%	0.00%
TOTAL VOLUME		**4611**	**6.2**	**16.8**	**0.93**	**88581**	**350.2**	**78.67**	**87666**	**0.69**	**9.7%**	

ANNEX 5

Hazen –Willam coefficients for different materials

Material	Coefficient - C -
ABS - Acrylonite Butadiene Styrene	130
Aluminum	130 - 150
Asbestos Cement	140
Asphalt Lining	130 - 140
Brass	130 - 140
Brick sewer	90 - 100
Cast-Iron - new unlined (CIP)	130
Cast-Iron 10 years old	107 - 113
Cast-Iron 20 years old	89 - 100
Cast-Iron 30 years old	75 - 90
Cast-Iron 40 years old	64-83
Cast-Iron, asphalt coated	100
Cast-Iron, cement lined	140
Cast-Iron, bituminous lined	140
Cast-Iron, sea-coated	120
Cast-Iron, wrought plain	100
Cement lining	130 - 140
Concrete	100 - 140
Concrete lined, steel forms	140
Concrete lined, wooden forms	120
Concrete, old	100 - 110
Copper	130 - 140
Corrugated Metal	60
Ductile Iron Pipe (DIP)	140
Ductile Iron, cement lined	120
Fiber	140
Fiber Glass Pipe - FRP	150
Galvanized iron	120
Glass	130
Lead	130 - 140
Metal Pipes - Very to extremely smooth	130 - 140
Plastic	130 - 150
Polyethylene, PE, PEH	140
Polyvinyl chloride, PVC, CPVC	150
Smooth Pipes	140
Steel new unlined	140 - 150
Steel, corrugated	60
Steel, welded and seamless	100
Steel, interior riveted, no projecting rivets	110
Steel, projecting girth and horizontal rivets	100
Steel, vitrified, spiral-riveted	90 - 110
Steel, welded and seamless	100
Tin	130
Vitrified Clay	110
Wrought iron, plain	100
Wooden or Masonry Pipe - Smooth	120
Wood Stave	110 - 120

Source: Good calculators